Improving EEG Classification Accuracy of Single Limb Imaginary Movements by Leveraging an Established EMG Pattern Recognition Scheme

by

Mojgan Tavakolan

M.Eng., Simon Fraser University, 2010

Thesis submitted in Partial Fulfillment of the
Requirements for the Degree of
Doctor of Philosophy

in the
School of Engineering Science
Faculty of Applied Science

SIMON FRASER UNIVERSITY

Fall 2017

Approval

Name: **Mojgan Tavakolan**
Degree: **Doctor of Philosophy**
Title: **Improving EEG Classification Accuracy of Single Limb Imaginary Movements by Leveraging Established EMG Pattern Recognition Scheme**

Examining Committee: Chair: **Dr. Ash Parameswaran**

Professor

Dr. Carlo Menon, PEng
Senior supervisor
Professor _____

Dr. Teresa Cheung
Supervisor
Assistant Professor _____

Dr. Lara Boyd
Supervisor
Professor _____

Dr. Faranak Farzan
Internal Examiner
Assistant Professor _____

Dr. Rene Mayorga
External Examiner
Professor _____

Date Defended: September 27, 2017

Abstract

Brain-computer interfaces may enable the collaboration between human and machines. They can in fact potentially translate the electrical activity of the brain to understandable commands to operate a machine or a device.

In this thesis, a method is proposed to improve the accuracy of a BCI by leveraging an established electromyography (EMG) pattern recognition scheme. Such a pattern recognition scheme extracts time-domain features, which include autoregressive (AR) model coefficients, root mean square (RMS), waveform length (WL) and classifies them using an optimized support vector machine (SVM) with a radial basis kernel function (RBF).

Upon validating that such a method can indeed process EMG signals to classify different fifteen movements of the arm with high accuracy (> 90%), this thesis investigates the possibility of implementing it for the design of a BCI based on electroencephalographic (EEG) signals. The discrimination of rest, imaginary grasp and imaginary elbow movement of the same limb was selected as test case to validate the designed BCI. This classification task is particularly challenging because imaginary movements within the same limb have close spatial representations on the motor cortex area.

The use of the proposed method was demonstrated to be suitable for identifying imaginary movements using EEG signal. In fact, the investigated method achieved an average accuracy of 91.8 % and 90 % for identifying the user intention corresponding to imaginary grasps and imaginary elbow movements (2-class BCI). An average classification accuracy of 74.2 % was achieved for classification of rest versus imaginary grasps versus imaginary elbow movements (3-class BCI).

The investigated method outperformed methods that are widely used in the BCI literature such as common spatial patterns (CSP), filter bank CSP (FBCSP), and band power methods. These results are encouraging and the proposed method could potentially be used in the future in BCI-driven robotic devices to assist individuals with impaired upper extremity functions in performing daily tasks.

Keywords: Brain-computer interface; Classification; Feature extraction; Support vector machines.

Acknowledgements

I would like to thank Dr. Carlo Menon for his leadership, support, counselling and encouragement throughout my PhD studies. He has given me a tremendous amount of feedback for improving on this study in the field of biomedical engineering.

I would also like to express my gratitude to all my colleagues and all individuals that helped me during my studies.

Table of Contents

List of Tables

List of Figures

List of Acronyms

AR	Autoregressive
BCI	Brain-Computer Interface
BP	Backpropagation
CSP	Common Spatial Patterns
ECOG	Electrocorticography
ECR	Extensor Carpi Radialis
ED	Extensor Digitorum
EEG	Electroencephalographic
EMG	Electromyography
ERD	Event Related Desynchronization
ERP	Event Related Potential
ERS	Event Related Synchronization
FBCSP	Filter Bank Common Spatial Patterns
FCU	Flexor Carpi Ulnaris
FES	Functional Electrical Stimulation
KNN	K-Nearest Neighbor
LDA	Linear Discriminant Analysis
MEG	Magnetoencephalography
MI	Motor Imagery
MI-ELBOW	Motor Imagery of Elbow Flexion and Extension
MI-GRASP	Motor Imagery of Grasp
MLP	Multilayer Perceptron
MVC	Maximum Voluntary Contraction
NN	Neural Networks
PL	Palmaris Longus
PS	Previous Study
RBF	Radial Basis Function
RMS	Root Mean Square
SMR	Sensory Motor Rhythm
SSVEP	Steady State Visual Evoked Potential
SVM	Support Vector Machine
WL	Waveform Length

Chapter 1. Introduction

1.1. Introduction

This chapter provides an overview of the necessary background knowledge for BCI research. The types of movements explored for interpretation by BCIs are discussed and the combination of motor imagery of grasping and elbow movements of the same arm are deduced to be novel to BCI literature to the best of the author's knowledge. The objectives of the research and outline of thesis are also discussed in this chapter.

1.2. Motivation

Brain-computer Interface (BCI) is a direct communication pathway between the brain and external electronic devices aiming at translating brain activities into control commands. In recent years, the use of BCI has been shown to be promising for detecting the users' intention and controlling robotic devices [1]. A BCI system detects electrical changes in brain and attempts to find patterns that are related to the thoughts or specific movements. Electroencephalographic (EEG) signals can be correlated to the tasks performed by an individual [2]. Such tasks include imagining motor movements [3], imagining speech [4] and mental computation [5].

Several different classification schemes with a variety of complexity and efficiency in different domains were suggested for EEG signal analysis and identifying the correlation with tasks performed [6, 7]. Palaniappan trained the Elman Neural Network by the resilient backpropagation (BP) and a classification accuracy of 86% was obtained [8]. Hema *et al.* employed a fuzzy classifier and extracted power of the spectral frequencies for classification of five mental tasks and an accuracy of 65% to 100% was obtained [9]. Diez *et al.* used empirical mode decomposition for feature extraction and classification accuracy of 87±5% was achieved when multilayer perceptron (MLP) network was implemented and an accuracy of 91±5% was obtained when linear discriminant analysis was used [10]. Huan and Palaniappan utilized MLP-BP and adaptive auto regression and classification accuracy of 81.80% was obtained [11].

Although there were several attempts, the detection of the task the user intends to perform is however still a field of research. It is not straightforward to apply existing BCI systems to control devices such as robotic assistive devices. The main reason is that these BCI systems can only recognize a limited number of mental tasks as control commands. Left hand, right hand, and foot motor imagery tasks are among the most frequently used motor imagery tasks in controlling BCI systems [12]. The task of detecting the intention or discriminating the motor imagery of different movements within the same limb is particularly challenging. This is due to the fact that these motor tasks activate regions that have close representations on the motor cortex area of the brain. To date, not many studies addressed this problem [13, 14].

Some of the studies look into the decoding of different wrist movements [15, 16]. The classification of four different imaginary wrist movements namely wrist extension, flexion, pronation, and supination were demonstrated in [17] and unfortunately, the accuracies achieved are not satisfactory (approximately 35%). There are BCIs that only classify two classes such as left versus right motor imagery or mostly rest versus motor imagery [18-22]. Existing multi-classes classification schemes do not result in acceptable classification accuracies using EEG signals. Therefore, a solution to identify multiple classes of the upper extremity is needed which potentially benefits the individuals with upper extremity impairment. A classification scheme is proposed in this thesis to improve the classification accuracies using EEG signals. The proposed classification scheme could potentially be used to identify the activities of the upper extremity.

1.3. Objectives

The overall goal of this thesis is to investigate the proposed classification scheme if it could provide references for further enhancing the recognition rate of EEG and make BCI more practical.

In previous study (PS) [23] performed by Dr. Xinyi Yong, a former member of the MENRVA research group nine different classification schemes which were combinations of nine different feature extraction and classification methods were used to discriminate

the different classes of EEG signals. The reported accuracy for each participant was the highest cross-validation accuracy obtained from one of the nine algorithms.

The goal of this thesis is to investigate if the proposed classification scheme, which extracts time-domain features, could lead to higher performance. The proposed time-domain feature extraction method is compared to widely used methods such as CSP, FBCSP and band power methods.

Motor imagery of grasping and elbow movements were chosen due to their potential use in controlling the robotic exoskeleton [24] developed in the MENRVA research lab. For example, the user could imagine elbow movements to move the robotic device close to a cup, and then imagine grasping movements to grab the cup.

In order to achieve the overall goal of the thesis, two research objectives are proposed and presented in the following sections.

Objective 1: Binary classification problem

The first objective of this thesis is to explore the feasibility of the classification scheme focusing on the binary classification of functional activities of the same upper limb. Binary classification is the task of classifying the EEG signal into two groups. Binary classification determines if a participant has motor movement intention or not – the classification result specifies the presence of the intention. This thesis, first investigates the binary classification of the following combinations (objective 1.1 and objective 1.2):

Objective 1.1: Rest versus motor imagery of grasp

Objective 1.2: Rest versus motor imagery of elbow flexion and extension

Objective 2: Multi-class classification problem

This second objective is to investigate the feasibility of utilizing EEG in a multi-class BCI system that discriminates EEG signals corresponding to rest or other imaginary of the functional movements within the same limb. This objective is set to

assess the possibility of designing a 3-class BCI that discriminates rest, imaginary grasp movements and imaginary elbow movements.

1.4. Outline of Thesis

The following chapters of this thesis are organized as follows:

- Chapter 2 briefly explains the anatomical structures of the brain and their functions.

- Chapter 3 summarizes the state of the art in the field of brain-computer interfacing.

- Chapter 4 presents the proposed classification scheme adopted from the electromyography (EMG) literature including feature extraction and classification method for upper extremity pattern recognition.

- Chapter 5 investigates the performance of the classification scheme in identifying multiple classes of the upper extremity using EMG signals. This chapter demonstrates how accurate the classification scheme is.

- Chapter 6 describes the experimental procedure including signal acquisition and analysis for different motor imageries.

- Chapter 7 presents the performance for predicting the neutral state of the brain versus the upper extremity gestures involved in a functional imagery movement.

- Chapter 8 presents recognition performance for the multi-class upper extremity imagery movements.

- Chapter 9 is dedicated to the comparison between the proposed approach and the more popular approaches for imaginary movement recognition.

- Chapter 10 draws the conclusion of the thesis and summarizes the work done toward achieving the objectives as well as the scientific contributions of the thesis.

The two objectives of the thesis are addressed in the following chapters:

- Objective 1 is addressed in chapters 7. Chapter 7 presents the optimal binary classification models and the corresponding classification results.

- Objective 2 is addressed in chapters 8. Specifically chapter 8 presents the optimal multi-class classification model for each participant. The obtained classification results of objective 2 are also presented in this chapter.

- Objective 1 and objective 2 are also addressed in chapters 9. In chapter 9 the obtained results of the proposed method are compared with the obtained results of the well-known methods.

1.5. Conclusion

This chapter introduced the limitations of current classification schemes. Same limb grasp and elbow motor imageries were selected in order to their potential use in controlling the robotic arm [24] developed in the MENRVA research lab to provide basic hand functionality and aid daily activities. The overall objective of the research was defined. The objective was split into two investigations and the purpose of each were detailed.

The next chapters provide some basic background knowledge and relevant terminology pertaining to the research. The design and implementation of the method used is documented and the consequential results are thereafter presented and discussed. Future work is briefly discussed and the research is concluded.

Chapter 2. Physiological Background

2.1. Introduction

Brain-computer interface research involves and integrates researchers from different fields including engineering, neuroscience, computer science and rehabilitation [25, 26]. Thus in order to contextualise this research, some basic background is provided in this chapter. This includes necessary terminology, relevant neural anatomical and physiological knowledge.

In this chapter the anatomical structures of the brain and their functions are briefly explained. Then the focus is on the brain generating electrical activities that can be recorded on the scalp.

2.2. The Brain

The supreme commander of the human body is the brain which governs the functions of various organs in the body. The brain can be divided into three major parts; cerebrum, cerebellum and brainstem [27] as illustrated in Figure 2.1.

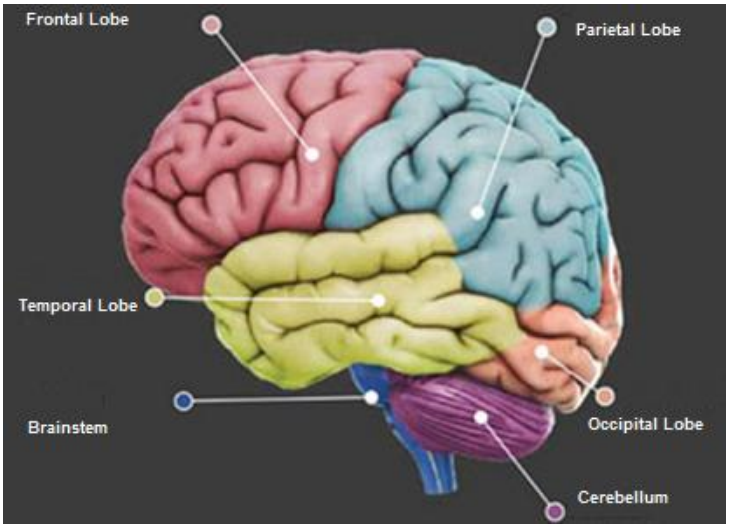

Figure 2.1: Anatomical areas of the brain [27].

2.2.1 Cerebrum

The cerebrum is the most important and largest part of the human brain. The cerebrum is generally associated with brain functions related to thoughts, movements, motor functions and emotions. The cerebrum is divided into two hemispheres, the left and right hemispheres. Each hemisphere has four lobes that are named after the bones that cover them: frontal lobe, parietal lobe, temporal lobe and occipital lobe (Figure 2.1).

A central sulcus separates the frontal and parietal lobes (see Figure 2.2). The precentral gyrus (region 1 in Figure 2.2) is located immediately anterior to the central sulcus, and it contains the primary motor area of the cerebral cortex. The postcentral gyrus (region 2 in Figure 2.2), located immediately posterior to the central sulcus, contains the primary somatosensory area of the central cortex.

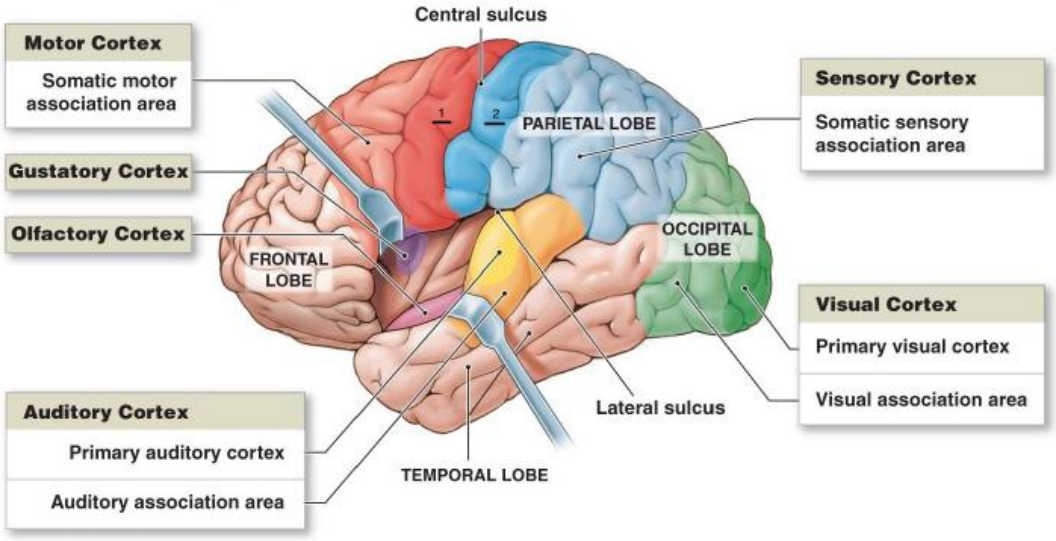

Figure 2.2: The brain. The cerebrum is divided into four lobes: frontal lobe parietal lobe, temporal lobe and occipital lobe. Region 1 and region 2 represent the primary motor area and the primary somatosensory area, respectively. Adapted from Pearson Education, Inc.

The primary motor area controls voluntary contractions of specific muscles of the body. The primary motor area and the primary somatosensory area, jointly called sensorimotor cortex. Over this region (Figure 2.3) the representation of human body muscles was mapped by Penfield and Rasmussen. This mapping was done by electrically stimulating the different areas of the sensorimotor cortex.The size of the area

is related to the importance and complexity of movement of a particular body muscle. It is possible to notice that more than half of the entire sensorimotor cortex is concerned with controlling the muscles of hand and speech (see Figure 2.3) [28].

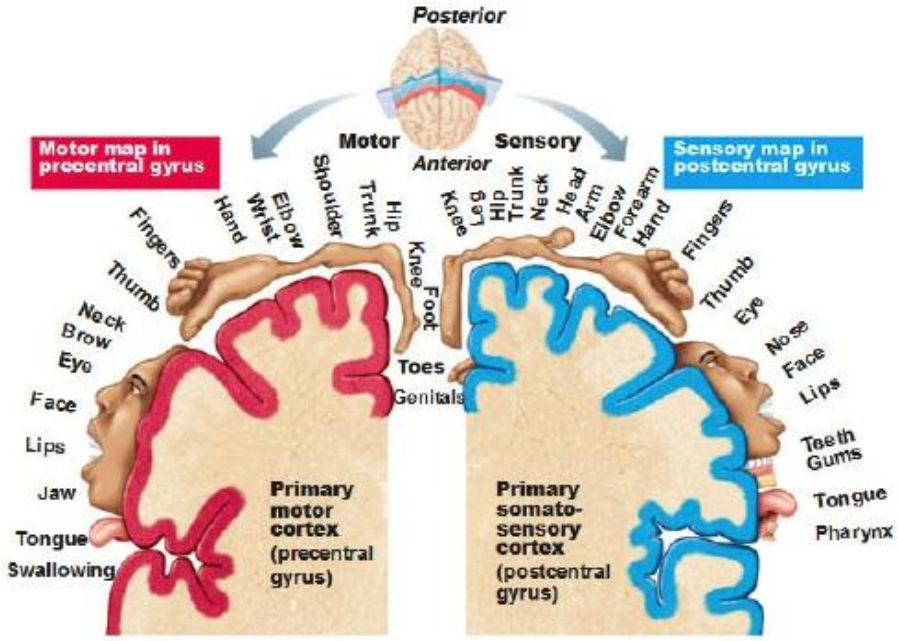

Figure 2.3: Homunculus: representation of the different body muscles over the sensorimotor cortex. Adapted from Antranik.org.

2.3. Human brains' neurophysiology

The human brain consists of about 100 billion nerve cells called neurons. The electrical charge of the brain is maintained by these neurons. Neurons share the same characteristics and have the same parts as other cells. The electrochemical aspect lets them transmit electrical signals and pass messages to each other. In general terms a neuron consists (Figure 2.4) of a cell body (soma) that contains the nucleus, an axon that carries the neuron's output in the form of action potentials and a dendritic tree that together with the soma, receives inputs from other elements through specialized structures called synapses.

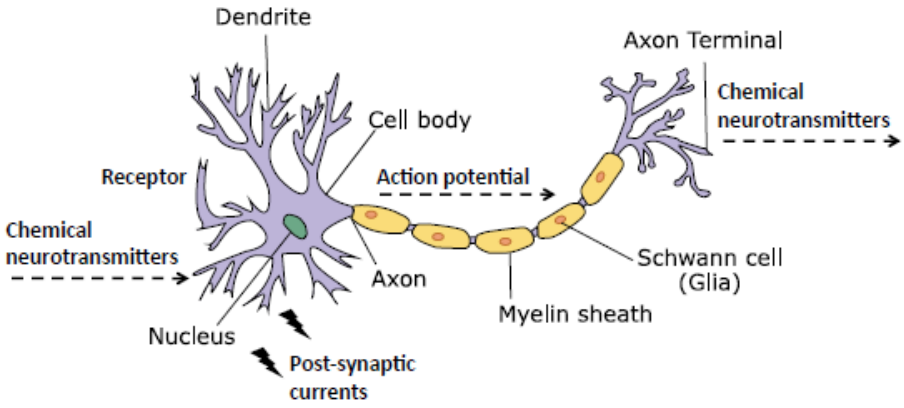

Figure 2.4: A simple structure of neuron.

The nucleus is the heart of the cell, providing it with instructions on what to do. The axon connects the nucleus of its own neuron to the dendrite of another neuron. Through the axon-dendrite link, neurons can communicate between each other.

2.4. EEG Recordings

Large populations of active neurons can generate electrical activity recordable on the scalp [29-31]. In the EEG measurement, the cerebral cortex is the most relevant structure as it is responsible for tasks such as movement, problem solving, processing of complex visual information and language comprehension. Due to its surface position, the electrical activity of the cerebral cortex has the greatest influence on EEG recordings.

2.4.1. Electrodes

A cap with a number of electrodes is placed on the user's head. Each electrode has a letter to identify the lobe and a number to identify the hemisphere location. The letters F, C, T, P and O stand for Frontal, Central, Temporal, Parietal and Occipital respectively. A "z" or zero refers to an electrode placed on the midline. Even numbers (2, 4, 6 and 8) refer to electrode positions on the right hemisphere, whereas odd numbers (1, 3, 5 and 7) refer to those on the left hemisphere.

Electrodes pick up the signal from the head surface. These scalp measurements detect potential changes over time in a basic electric circuit between an active electrode and a reference electrode. Many different physical references can be chosen, but vertex (Cz electrode) is the frequently used reference electrode. This signal is then amplified, digitalized and stored in a computer.

2.5. Neurophysiological phenomena

Neurophysiological phenomena may be used to extract information from scalp-recorded EEG signals. Such phenomena are generated consciously by the user (endogenus BCI), or unconsciously in response to an external stimulation (exogenous BCI). Exogenous BCIs are based on Event Related Potentials (ERPs), whereas endogenous BCIs are based on Sensory-Motor Rhythms (SMR). In the following paragraphs these neurophysiological phenomena are briefly exposed.

2.5.1 Event Related Potentials

Event-related potentials can be measured in the EEG before, during or after a certain event. Event-related potentials have a fixed time delay to the stimulus and their amplitude is usually much smaller than the ongoing spontaneous EEG activity. They can be detected by averaging many recordings time-locked to the event. The averaging cancels out the background activity, which is not synchronized with the stimulus and leaves only ERPs. P300 and Steady State Visual Evoked Potentials (SSVEP) are the commonly used ERPs.

2.5.2 Sensory-Motor Rythms

Sensory-Motor Rhythms are oscillatory activities observable in sensory-motor areas of the cortex. It is known that motor imagery, preparation for movement, or movement is usually accompanied by a decrease in the mu and beta rhythms over the sensorimotor cortex area especially the contra-lateral region [32, 33]. This decrease is also known as event-related desynchronization (ERD).A recent study suggested that the degree of this decrease might be quantitatively associated with an increase in neuronal activity [33]. Besides ERD, an increase in the beta rhythm also occurs after a motor

imagery or a movement is executed. This increase is known as event-related synchronization (ERS). Mu and beta rhythms are relevant in the scope of this thesis as imagery movement are associated with mu and beta rhythm desynchronization.

2.6. Conclusion

The theoretical background necessary to understand the anatomic and physiologic fundamentals of the brain were presented. Also, a brief description of the electroencephalography and its phenomenology was given. This is relevant information needed to contextualise the problem to decipher the EEG for different motor imageries using an EEG-based BCI. The next chapter is an overview of brain-computer interfaces.

Chapter 3. Brain Computer Interface

3.1. Introduction

This chapter summarizes the state of the art in the field of brain-computer interfacing. Section 3.2 describes a generalized BCI system and presents the main components along with their dependences and interconnections. Section 3.3 deals with the main techniques available to acquire brain signals. The following sections are about EEG signal feature extraction (Section 3.4) and classification (Section 3.5).

3.2. Generalized BCI system

A Brain-Computer Interface is a communication system that allows controlling an external device using signals measured from the brain. A BCI bypasses any muscle or nerve mediation and establishes a direct communication pathway from the human brain to the outer world. BCI systems aim to provide a means of communication and control for people who suffer from neuromuscular disorders or motor disabilities, such as spinal cord injuries, brainstem stroke, multiple sclerosis and limb amputations [2, 34-35]. BCIs could allow the use of assistive devices such as wheelchairs, prosthetics and orthotics in order to improve the quality of life of such individuals [35].

3.2.1 BCI Components

In general a BCI system consists of the following main components, as depicted in Figure 3.1:

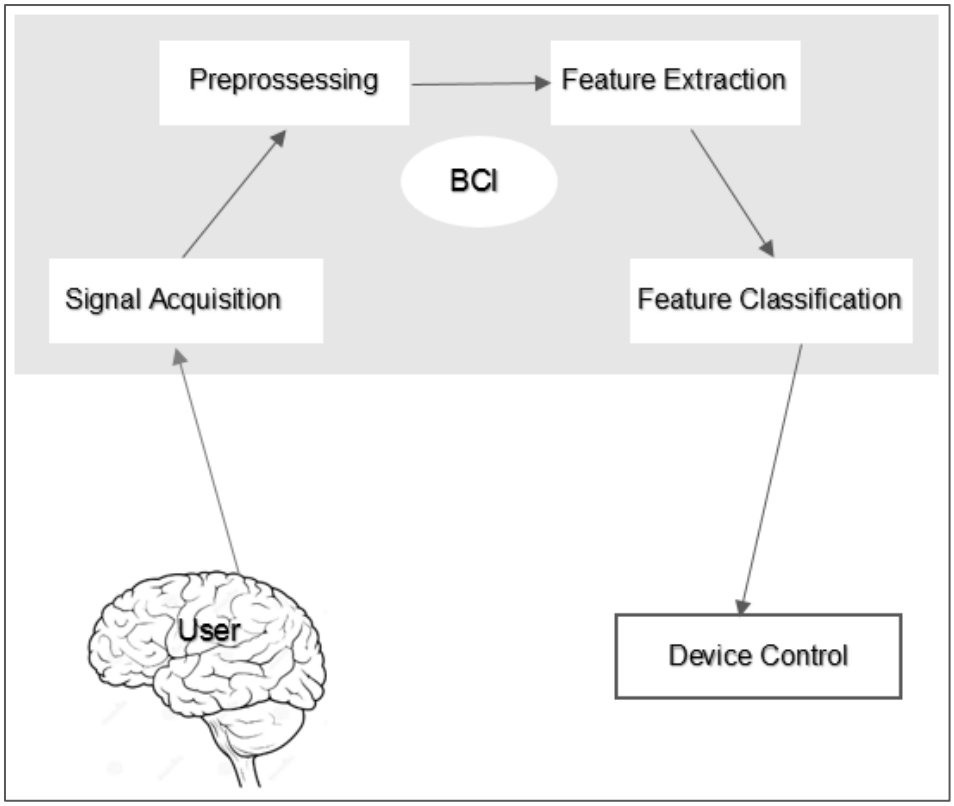

Figure 3.1: Generalized BCI system

3.2.1.1 Signal Acquisition

In the first stage a signal related to neuronal activity is recorded from the brain. This signal may be acquired with several techniques having different spatial and temporal resolutions, different levels of invasiveness and different characteristics of the recording equipment.

3.2.1.2 Processing and Translation

Signal processing and translation is the most important component of any BCI system.Its goal is to convert signals recorded from the brain into a control signal suitable for an external device. In the processing part the signal is filtered and relevant features are extracted in order to discriminate relevant brain activities. In the translation part these features are used to generate a continuous or discrete control signal.

BCI analysis can be done online or offline [34]. In the case of offline analysis, data is recorded and techniques are applied to the data thereafter [34]. Methods that appear promising offline can be executed by extensive online testing, where the individual's neural signals are analyzed in real-time [34, 35].

Following sections describes the mentioned BCI components in more detail.

3.3. Signal Acquisition

There are several ways to acquire signals from the brain, all falling into two main categories: invasive and non-invasive techniques. Invasive BCIs use activity recorded by brain implanted micro-electrodes, whereas non-invasive BCIs use brain signals recorded from outside the body boundaries.

Invasive recording methods either measure the neural activity of the brain within the cortex or on the cortical surface (electrocorticography, ECoG). While having strong advantages in terms of signal quality, the invasive methods require delicate and risky surgeries with all the problems related to protection from infections and stability of implants.

Non-invasive methods based on electrical brain activity are mainly divided into two categories: magnetoencephalography (MEG) and electroencephalography (EEG). MEG is sensitive to the magnetic fields induced by the electric currents in the brain. MEG provides a precise spatial resolution (about 5 millimeters) and a good temporal resolution, but the recording equipment is bulky and expensive. To date, this method is used only in laboratory settings and is consequently not suitable for controlling a BCI in the patient's home environment.

Electroencephalography makes use of electrodes on the scalp to sense the electrical fields. EEG recordings provide good temporal resolution (in the order of milliseconds) but suffer of a poor spatial resolution (in the order of centimeters). This limitation in signal localization is mainly due to the diffusive effects caused by all intermediate tissues between the brain cortex and the scalp. However EEG is still the preferred choice for non-invasive BCIs, because of its fine temporal resolution, ease of

use and portability. Electroencephalography is acquisition technique adopted in this thesis.

3.4. Feature Extraction

The main goal of a BCI is to discriminate the user's intentions by means of brain activity. For this purpose relevant features need to be extracted from the EEG so that neurophysiological phenomena underlying the recorded brain activity can be identified and successively translated into control signals. These features may be extracted in the time, frequency or spatial domain.

3.4.1 Time-Domain Features

Features extracted in the time domain relate how the amplitude of the EEG signal vary to specific tasks performed by the user. In order to separate relevant information from background activity, filtering and windowing techniques are normally adopted for time-domain features. Since time-domain features are adopted in this thesis a more detailed explanation of these features is reported in Section 4.3.1.

3.4.2 Frequency Domain Features

Frequency domain features are related to changes in the oscillatory activity of the EEG signal. Such changes may be generated by the user concentrating on a specific mental task. Frequency domain features are employed with BCI systems.

3.4.3 Spatial Domain Features

The main goal of spatial domain features is to combine information coming from different EEG channels in order to identify patterns in brain activity related to different neurophysiological phenomena. Several spatial filtering techniques have been employed for this purpose, the most common being CSP, PCA and ICA. Spatial features were widely adopted for motor-imagery. Indeed neuronal activity is recorded from multiple electrodes and spatial variations of EEG potentials have been proven to be source of

discriminative information. Since the proposed time-domain features are compared with these widely used features, more detailed explanation is reported in Section 6.6.

3.5. Classification

The classification of EEG signals plays an important role in BCI research. Classification is the procedure of assigning one of a given number of categories to a given piece of input data. There are two types of classification: supervised and unsupervised classification. In supervised classification, observations of a set of data are associated with class labels, whereas in unsupervised classification, observations are not labelled and are not assigned to a known class.

3.5.1 Supervised Classification

Supervised classification is preferred in the majority of BCI research. The algorithms of supervised classification deal with data that class label information is given within the dataset. Data with class labels are used for training the classifier. In this type of classification algorithm, a supervisor instructs the classifier during the construction of the classification model. Supervised classification schemes assume that a set of training data are provided, consisting of a set of instances that are properly labelled.

In the supervised approach, there are pairs of labelled data in the training dataset which can be mathematically expressed as: D = {(*x1*, *t1*), (*x2, t2*),....., (*xN*, *tN*)}. *x1*, *x2*,.....,*xN* are the observations and *t1*, *t2*,.....,*tN* are the class labels (targets) of the observations. In this type of classification, the aim is to find the transformation between the feature space *X* and the class label space *T*. For example for the case of a binary classification problem (objective 1 of this research), the classes are divided into two categories, such as the target and non-target classes. In binary classification the existence of a target is detected. For the case of a multiclass classification problem (objective 2 of this research), the classes are divided into *n* categories and a one-versus-one strategy was applied. A more detailed explanation is reported in Section 4.3.2.

Support vector machine (SVM), Linear discriminant analysis (LDA), Decision trees, K-nearest-neighbor (KNN) algorithms and Neural networks (NN) are the examples

of algorithms used in supervised classification procedure for predicting categorical labels. In this research, a supervised procedure was used in the classification.

In the BCI system developed for this thesis, the classification is performed by means of the support vector machine. Section 4.3.2 describes in details the classification model applied and provides motivations for adopting this classifier.

3.5.2 Unsupervised Classification

The unsupervised classification procedure involves grouping data into categories based on some measure of inherent ability. In unsupervised learning, no information about the class labels is available. This procedure attempts to find patterns in the data that can then be used to determine the correct class label for new data instances. The common algorithms used in unsupervised classification are K-means clustering, Hierarchical clustering and Hidden Markov Models.

3.6. Conclusion

Some background knowledge on EEG acquisition and BCIs is outlined in this chapter. This chapter introduced two types of classification used in control. This is relevant information needed to categorize the EEG signals using EEG-based BCIs. The next chapter details the design and implementation of the proposed method including feature extraction and classification to perform the investigations.

Chapter 4. Rationale and Investigated Classification Scheme

4.1. Introduction

This chapter presents the established classification scheme adopted from EMG literature. This approach is based on feature extraction (section 4.3.1) and classification (section 4.3.2). The classification scheme presented in this chapter is utilized to address objectives 1 and 2 of this thesis.

4.2. Rationale

There is a significant power increases in EEG during both motor execution and motor imagery [37]. EEG measurements during motor execution and motor imagery are correlated with EMG activity and EMG measurements [37]. In this chapter the pattern recognition schemes was presented to improve EEG classification accuracy of single limb movements by exploring and then leveraging established EMG pattern recognition scheme.

4.3. The classification scheme

The classification scheme is the established pattern recognition scheme proposed in EMG literature [38-44]. In this section the classification scheme including feature extraction and classification method are explained and followed by a case study which is a practical evidence of capability of such a scheme in the EMG field of use. The combination of single limb motor imagery of grasping and elbow movements which is deduced to be novel to BCI literature was used for classification. No time-domain BCI research exploring these imagery movements was found. This approach is based on feature extraction and support vector machine classification. The relevant features were extracted and translated into control signals.

4.3.1 Feature extraction

Feature extraction highlights important information and eliminates redundant or non-informative data. Feature extraction transforms the signals to a feature vector. In this study, time-domain features that are computed based on the signals' amplitudes were used. These features require no transformation or complex calculation [45]. The first extracted feature set consists of autoregressive (AR) model coefficients. The mathematical representation of an AR model is expressed by (1):

$$t_n = \sum_{i=1}^{p} a_i^p t_{n-i} \tag{1}$$

where {a for i = 1,. . . , p } are AR model coefficients and p is the model order. AR models the data such that the current sample is a weighted linear combination of its previous samples and thus, provides information regarding the previous samples.

The second feature set is waveform length (WL), which is the cumulative length of the waveform over the segment. This feature provides a measure of the waveform amplitude, frequency, and duration all within a single parameter [46]. It can be mathematically represented by (2):

$$y = \sum_{i-1}^{N} \left|\Delta w_i\right| = \sum_{i-1}^{N} \left|w_i - w_{i-1}\right| \tag{2}$$

where w_i is the amplitude of the i^{th} sample and N is the number of samples.

The third extracted feature set is root mean square (RMS). This feature provides information regarding the amplitudes of the signals. The feature is computed by (3):

$$RMS_{rms} = \sqrt{\frac{r_1^2 + r_2^2 + \ldots + r_n^2}{n}} \tag{3}$$

where r_i is the amplitude of the i^{th} sample and n is the number of samples.

The signals were segmented using a window size of one second. For each segment, the time domain features were extracted from each channel. AR generated four features and RMS and WL provided one feature for each channel respectively.

4.3.2. Classification

Classification is a popular approach in BCI research. Classification was used to identify patterns of brain activity and to translate these patterns into control commands. SVM is an efficient state-of-the-art classifier. SVM was used as a classifier. SVM finds discriminant hyper-planes that separate the data that belong to different classes with the maximum possible margin [47]. Maximizing the margins increases the generalization capabilities of the SVM classifier. In its general formulation, SVM [47] requires solving the following optimization problem:

$$\min_{w} \quad \frac{1}{2}\|w\|^2 + c\sum_{i=1}^{N} \xi_i \tag{4}$$

$$\text{subject to} \quad \begin{matrix} t_i\ y(x_i) \geq\ 1-\xi_i, \quad i = 1,\dots,N \\ \xi_i \geq 0 \end{matrix} \tag{5}$$

Where *N* is the number of data points, x_i is the vector representing a data point, t_i is the label associated with a data point, *y* is the learned model, *w* is the vector representing adaptive model parameters, ξ_i is the slack variable and *c > 0* is the penalty factor.

A linear SVM can make nonlinear decision boundaries by using the 'kernel trick'. It is generally done by mapping the data to higher dimensionality space, with the help of a kernel function [47]. SVM supports well-known kernels such as the polynomial, linear and radial basis function (RBF) to extend SVM for classification. The mathematical representation of the RBF, linear and polynomial kernel is respectively given by (6), (7) and (8):

$$k(x_i, x_j) = \exp(-\gamma \left\|x_i - x_j\right\|^2) \ , \ \gamma > 0 \tag{6}$$

$$k(x_i, x_j) = \ (\ \gamma.x_i.x_j + r)^d, \ \gamma > 0 \tag{7}$$

$$k(x_i, x_j) = x_i . x_j \quad (8)$$

where *r, d* and γ are kernel parameters and x_i, x_j are training vectors.

RBF was selected as the kernel function. The RBF kernel nonlinearly maps samples into a higher dimensional space. RBF has the least number of hyper-parameters compared to other kernel function such as polynomial kernel function [48]. Thus, it's computationally less expensive.

To optimize the performance of the classifier, it is crucial to find the optimal values for the cost (*c*) and the kernel parameter gamma (γ). The penalty weight *c*, acts like a regularization parameter that controls the misclassification rate of the training data and the kernel parameter gamma γ, is the convergence tolerance. The optimal values of these parameters were obtained from a grid search along with 10-fold cross-validation [49]. The data set was randomized and divided into ten folds. Nine of the folds were used to set up the classifier and the remaining one fold was used to test the classifier. This procedure was repeated for ten times [49]. The values of the parameters that resulted in the highest cross-validation accuracy were selected as the optimal pattern recognition model. The cross-validation procedure could help prevent over-fitting.

To achieve multiclass classification using SVM, one-versus-one strategy was employed [49]. In the one versus one voting scheme, *n (n−1)/2* binary classifiers for *n*-way multi-class problem are trained. During testing, all the binary classifiers are applied to an unseen sample and the class that receives the highest number of votes wins [49]. More specifically, every classifier assigns the data to one of the two classes [49]. Then, the assigned class receives one vote. The class that receives the highest number of votes is selected as the final class. In this case, *n* = 3 and for each 3-class classification problem, 3 binary classifiers were set up.

In a three-class classification problem, the output of the classifier had one of the three discrete states '0', '1', or '2' and was not a continuous function. The logical states '1' and '2' indicated the user's intention to activate a device (e.g. a robotic arm). The logical state '0', on the other hand, implied that the user did not intend to activate the system.

4.4. Conclusion

A method aimed at improving the interpretation of EEG is presented in this chapter. It is designed to allow the differentiation of EEG for different types of imagery movements and its general structure was applied to investigations of this thesis.

Chapter 5. A Case Study with EMG

5.1. Introduction

The proposed classification scheme provides high accuracy in identifying multiple classes of the upper extremity using EMG signals. The following case study in this chapter shows how accurate is the classification scheme. This chapter is an attempt to validate the use of the SVM classification approach to be used later on the BCI method. This chapter validates the hypothesis that, although there are significant neurological and physical changes occurring in humans while ageing, the proposed method could potentially be used by hand assistive devices controlled by the older people.

The content of this chapter was slightly modified from what first appeared in print in:

Tavakolan, M., Xiao, Z. G., & Menon, C. (2011). A preliminary investigation assessing the viability of classifying hand postures in seniors. *Biomedical engineering online*, *10*(1), 1.

5.2. Abstract

Surface electromyography (sEMG) controlled assistive devices for the upper extremities could potentially be used to augment seniors' force while training their muscles and reduce their fear of frailty. In fact, these devices could both improve self-confidence and facilitate independent leaving in domestic environments. The successful implementation of sEMG controlled devices for the elderly strongly relies on the capability of properly determining seniors' actions from their sEMG signals. In this research we investigated the viability of classifying hand postures in seniors from sEMG signals of their forearm muscles.

Nineteen participants, including seniors (70 years old in average) and young people (27 years old in average), were recruited for this study and sEMG signals from four of their forearm muscles (i.e. Extensor Digitorum, Palmaris Longus, Flexor Carpi

Ulnaris and Extensor Carpi Radialis) were recorded. The feature vectors were built by extracting features from each channel of sEMG including autoregressive model coefficients, waveform length and root mean square. Multi-class support vector machines was used as a classifier to distinguish between fifteen different essential hand gestures including finger pinching.

Classification of hand gestures both in the pronation and supination positions of the arm was possible. Classified hand gestures were: rest, ulnar deviation, radial deviation, grasp and four different finger pinching configurations. The obtained average classification accuracy was 90.6% for the seniors and 97.6% for the young participants. The obtained results proved that the pattern recognition of sEMG signals in seniors is feasible for both pronation and supination positions of the arm and the use of only four EMG channel is sufficient.

5.3. Background

Improving independent living of seniors and maintenance of their autonomy are compelling research goals for our society. Some simple activities of daily living such as opening and closing the screw cap of a bottle or turning a tap handle can be difficult tasks for a senior. By increasing the age, the skeletal muscles lose their strength [50]. In order to do every day simple operations, seniors would need using assistive devices that could provide an additional force for their hand movements and also train their muscles [51].

A compelling challenge in the development of assistive devices is how to acquire information from input signals that provide us with the information regarding the action the user is undertaking. Acquiring the input signals from the neurological activity of the user would provide us with the desired information. sEMG is a suitable technique for evaluating and measuring the electrical activity produced by skeletal muscles and can also provide us with important information regarding neuromuscular disorders [52].Using sEMG, we are able to detect the electrical signals generated by muscle cells when they are neurologically or electrically activated and if we interpret this information correctly, it can guide us towards the intention of the user [51, 52].

EMG signals have been considered to control prosthetic hands and assistive devices. Different prosthetic hands have been prototyped including the Smart Hand [53] and the Cyber Hand [54]. Some EMG driven prostheses have also been commercialised; examples are the Otto Bock's Sensor Hand Speed [55] and the iLimb [56]. In the mentioned researches, the goal was to obtain a prosthetic hand that could perform movements similar to a human hand. A challenging part in the development of these prosthetic hands is the design of an intuitive control achieved by detection and interpretation of the user's neurological activity [43, 57]. Whether used for controlling prosthetic, rehabilitative or assistive devices, sEMG signals should be processed to identify the intention of the user.

One of the main challenges related to the processing and classification of sEMG is related to the synergistic use of upper extremity muscles. For example, raising the shoulder to lift the forearm results in forearm signal changes [43]; similarly, contracting the index finger results in co-contraction of forearm muscles [58-60].

Different pattern recognition techniques have been used for classification of sEMG and identification of hand gestures in young participants [61, 62]. For example, multilayer perceptron [63, 64], SVM [9, 65-68], hidden markov model [69], neural networks [70], bayesian classifier [71] and fuzzy classifier [72-74] techniques have been proposed. Multiple features have been investigated including AR model coefficients [70,72,74-75], mean absolute value [75,76], slope sign changes [77,78], zero crossings [75-77], waveform length [77,78] and wavelet packet transform [79].

Most of the research has been performed with populations involving young healthy participants and amputees. Little research has however been carried out to assess if aging prevents a successful sEMG classification, which is needed to control assisted devices developed to augment force and reduce fear of frailty in the older people. It should be noted that there are significant neurological and physical changes occurring in humans while ageing [80]. This study therefore focuses on assessing the viability of classifying hand postures in seniors.

5.4. Methods

5.4.1 Data collection

A custom rig was used to measure hand force and torque exerted by the participants. The rig (see Figure 5.1) consisted of a force sensor (Futek LCM-300) which measured contraction force. This sensor was placed between two plastic halves, which formed together a semi-sphere to enable the participants to comfortably hold the rig with their hand. These two plastic halves were connected to a metallic platform through a torque sensor (Transducer Techniques TRT-100) that recorded torque produced by the participant while performing ulnar or radial deviation movements.

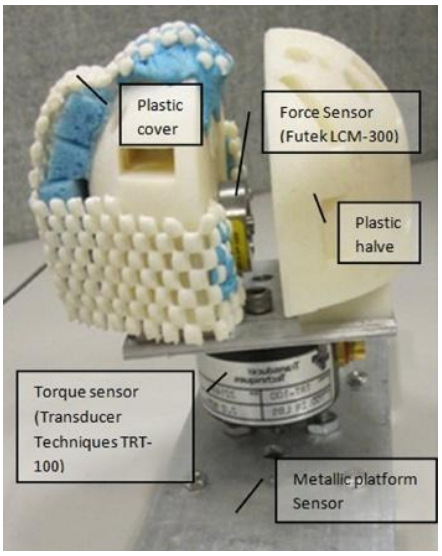

Figure 5.1: Custom rig.

Guidelines presented in the sEMG for the non-invasive assessment of muscles (SENIAM) project [81] were followed to obtain a fine skin contact with the electrodes. According to these guidelines, the skin was cleaned with an alcohol swab and electrodes were placed at the locations shown in Figure 5.2. sEMG electrodes were attached to the participants' forearms using medical adhesive bands that made the electrodes' active faces adhere the skin.

sEMG signals were recorded from the following four muscles in order to detect movement of wrist and fingers [82]: Extensor Digitorum (ED), Palmaris Longus (PL), Flexor Carpi Ulnaris (FCU) and Extensor Carpi Radialis(ECR). Function of each muscle

is summarized in Table 5.1. sEMG signals were acquired through a Noraxon system (Myosystem 1400L). A data acquisition board from National Instruments (USB-6289) was used in this study for acquiring both the sEMG signals and the data obtained from the custom rig used to measure hand force and torque. Since the EMG signal has usable energy in the 0-500 Hz range [83], the acquired sEMG signal was digitized at 1024 samples per second and stored on a computer through an application developed in LabVIEW software. The developed LabVIEW application also had a graphical interface to enable participants visualizing force they were exerting during the tests. For each participant, the maximum force exerted to the rig was used to define the participant's maximum voluntary contraction (MVC). According to [84], the applied force should not exceed 40-50% of the MVC in order to prevent upper extremity musculoskeletal injuries. For this reason, all the protocols were defined to prevent exceeding this limit.

Figure 5.2: Location of surface electrodes on the forearm.

5.4.2 Protocol

12 seniors (70 years old on average) and 7 young participants (27 years old on average) participated in this study. The Office of Research Ethics, Simon Fraser University approved this study and each participant signed a consent form. Each participant followed the eight predefined protocols summarized in Table 5.2. These protocols were defined to simulate simple activities of daily living involving the wrist and fingers such as opening and closing the screw cap of a jar or grasping an object. The identified protocols considered a combination of several hand movements including grasping, finger pinching, wrist ulnar/radial deviation and forearm pronation/supination. Each participant started at rest position as shown in Figure 5.3(a).

In protocol A, as shown in Figure 5.3(b), the participant was asked to squeeze the custom rig with maximum force in pronation position of the arm for two times. The recorded maximum force was used to define MVC for squeezing.

In protocol B, as shown in Figures 5.3(c)-(d), the participant was asked to apply maximum torque in ulnar and radial deviation for two times (pronation position of the arm). Maximum torques for ulnar and radial deviations were used to identify ulnar/radial MVCs.

In protocol C, the participant was asked to squeeze the custom rig at 50% of her/his MVC for 5 seconds (pronation position of the arm). The participant repeated this protocol three times. Using the graphical interface of the developed LabVIEW application, the participant had visual feedback for the force applied to the custom rig.

In protocol D, the participant was asked to alternate radial and ulnar deviation for 5 seconds at 50% of MVC (pronation position of the arm). The participant repeated this procedure three times.

In protocol E, as shown in Figures 5.3(e)-(h), the participant pinched the force sensor firstly with thumb and index finger, secondly with thumb and middle finger, thirdly with thumb and ring finger, and finally with thumb and little finger (pronation position of the arm). The pinching was repeated two times for each combination of fingers.

Table 5.1: Muscle function

Muscle	Function
FCU	Assists in wrist flexion with ulnar deviation
PL	Assists in wrist flexion
ED	ED Assists in extension of four fingers and the wrist
ECR	ECR Assists in extension and radial abduction of the wrist

Table 5.2: Protocols

Protocols	Definitions	Arm position
Protocol A	Apply maximum force by squeezing the custom rig two times.	Pronation
Protocol B	Apply maximum torque for radial deviation two times and then apply maximum torque for ulnar deviation two times.	Pronation
Protocol C	Apply 50% MVC force while squeezing for three seconds. Repeat for three times.	Pronation
Protocol D	Apply 50% MVC torque for alternate radial and ulnar deviation for three seconds. Repeat for three times.	Pronation
Protocol E	Pinch two times with a comfortable force using thumb and index finger, then two times using thumb and middle finger, then two times using thumb and ring finger and finally two times using thumb and little finger.	Pronation
Protocol FC	Apply 50% MVC force while squeezing for three seconds. Repeat for three times.	Supination
Protocol FD	Apply 50% MVC torque for alternate radial and ulnar deviation for three seconds. Repeat for three times.	Supination
Protocol FE	Pinch two times with a comfortable force using thumb and index finger, then two times using thumb and middle finger, then two times using thumb and ring finger and finally two times using thumb and little finger.	Supination

In Protocols FC, FD and FE (see Figures 5.4(a)-(h)), each participant started at rest position and repeated protocols C, D and E but with their arm in supinated position. Figure 5.5 presents the output recorded by the force and torque sensors for one of the participants following protocols A, B, C and D. Figure 5.6 presents a sample output of the force and torque sensors related to protocols E, FC, FD and FE.

Protocols A and B (see Table 5.2) were followed to record the maximum torque produced by the user. Protocols C, D, E, FC, FD, and FE were instead used to generate data for the formation of the different hand gesture classes summarized in Table 5.3. Specifically, protocols C, D and E enabled extracting data for classification purpose in the pronation position of the arm (classes 2-8 in Table 5.3) whereas protocols FC, FD and FE were used to extract data for classification in the supination position of the arm (classes 9-15 in Table 5.3).

5.4.3 Feature Extraction and Classification

Signals recorded from the Noraxon measurement system were processed in MATLAB for feature extraction of the raw sEMG input. Three types of features including waveform length, RMS and AR model coefficients were extracted. Specifically waveform length and RMS provided one feature each, whereas AR model coefficients provided four features for each channel. The features were extracted and classified as explained in the previous sections 4.3.1 and section 4.3.2.

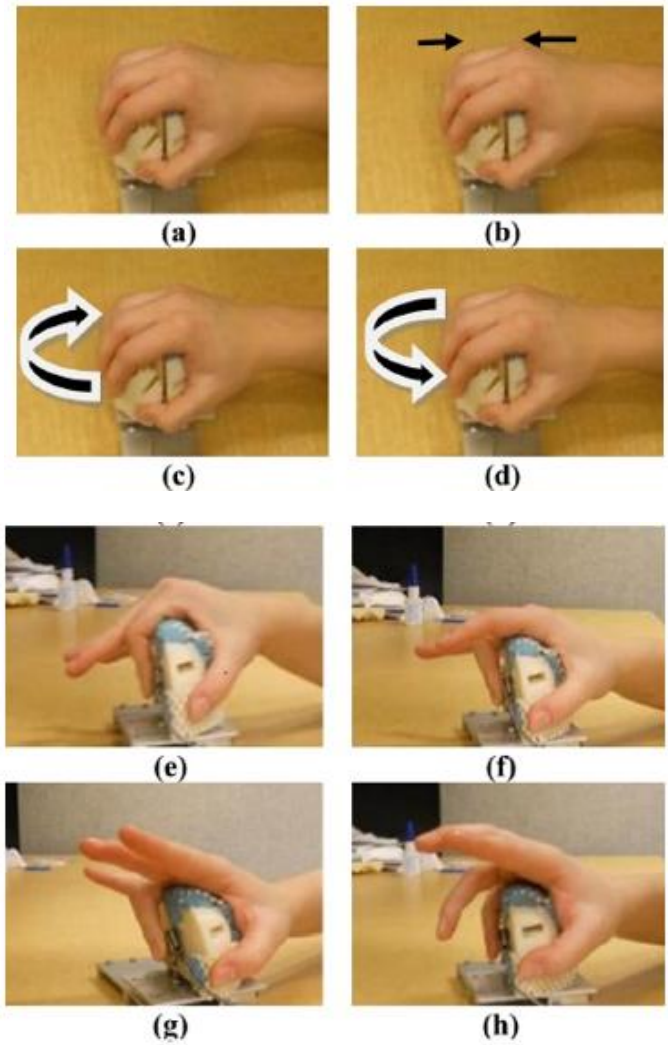

Figure 5.3: Hand gestures and motions chosen for classification in the pronation position of the arm. (a) rest, (b)grasp, (c) ulnar deviation, (d) radial deviation, (e)finger pinching: index finger, (f) finger pinching: middle finger, (g) finger pinching: ring finger, (h) finger pinching: little finger.

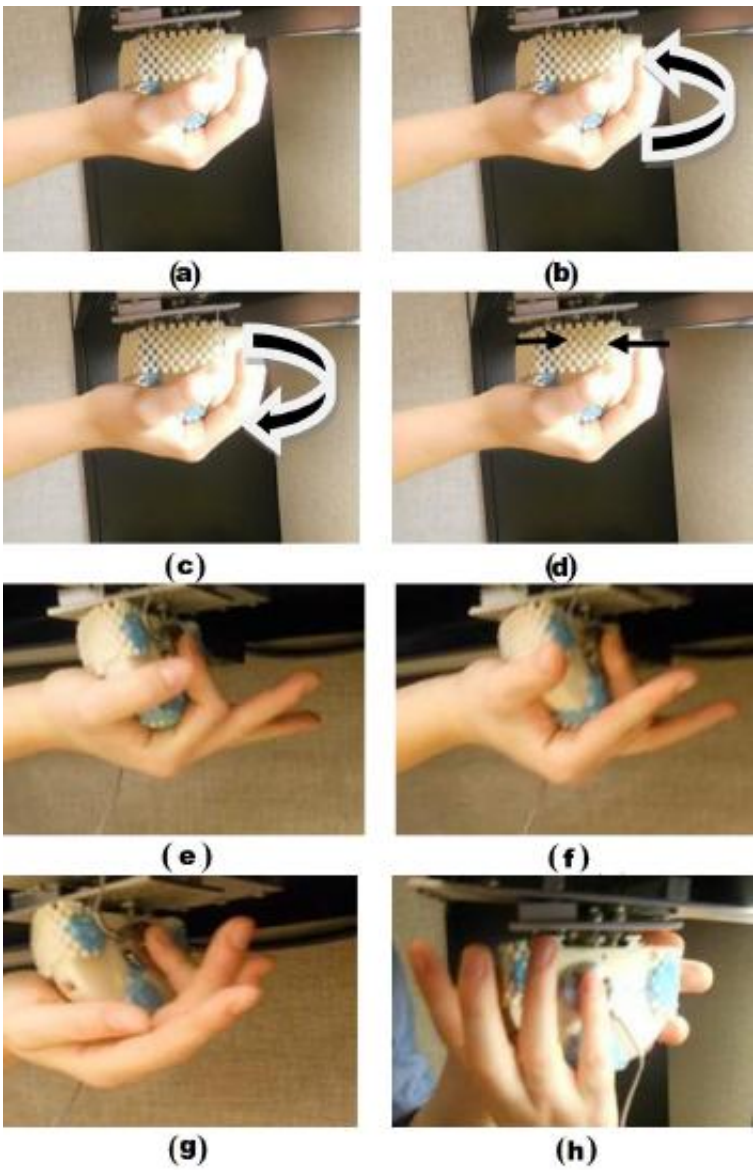

Figure 5.4: Hand gestures and motions chosen for classification in the supination position of the arm. (a) rest, (b) radial deviation, (c) ulnar deviation, (d) grasp, (e) finger pinching: index finger, (f) finger pinching: middle finger, (g) finger pinching: ring finger, (h) finger pinching: little finger.

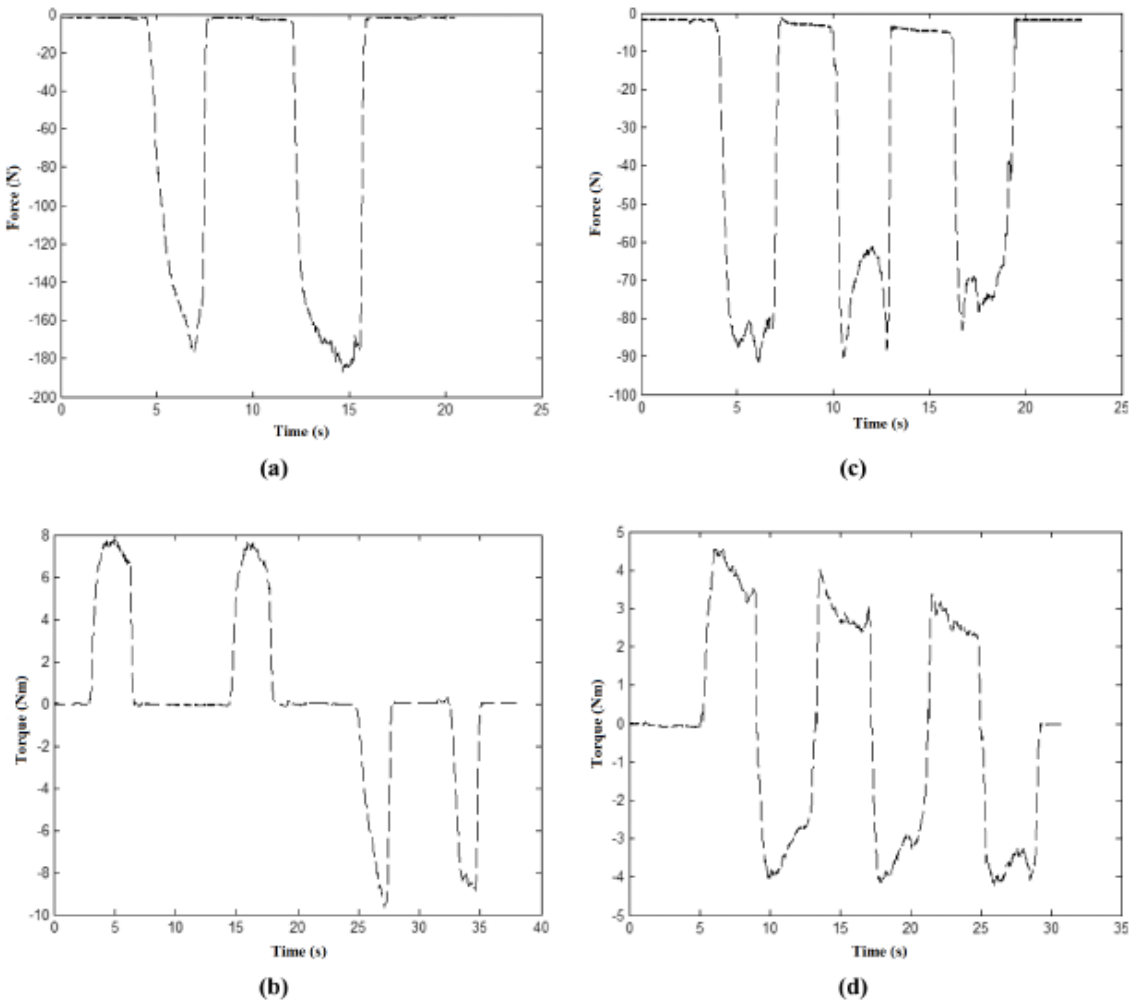

Figure 5.5: Forces and torques representing predefined protocols A, B, C and D. (a) Protocol A, (b) Protocol B, (c) Protocol C and (d) Protocol D.

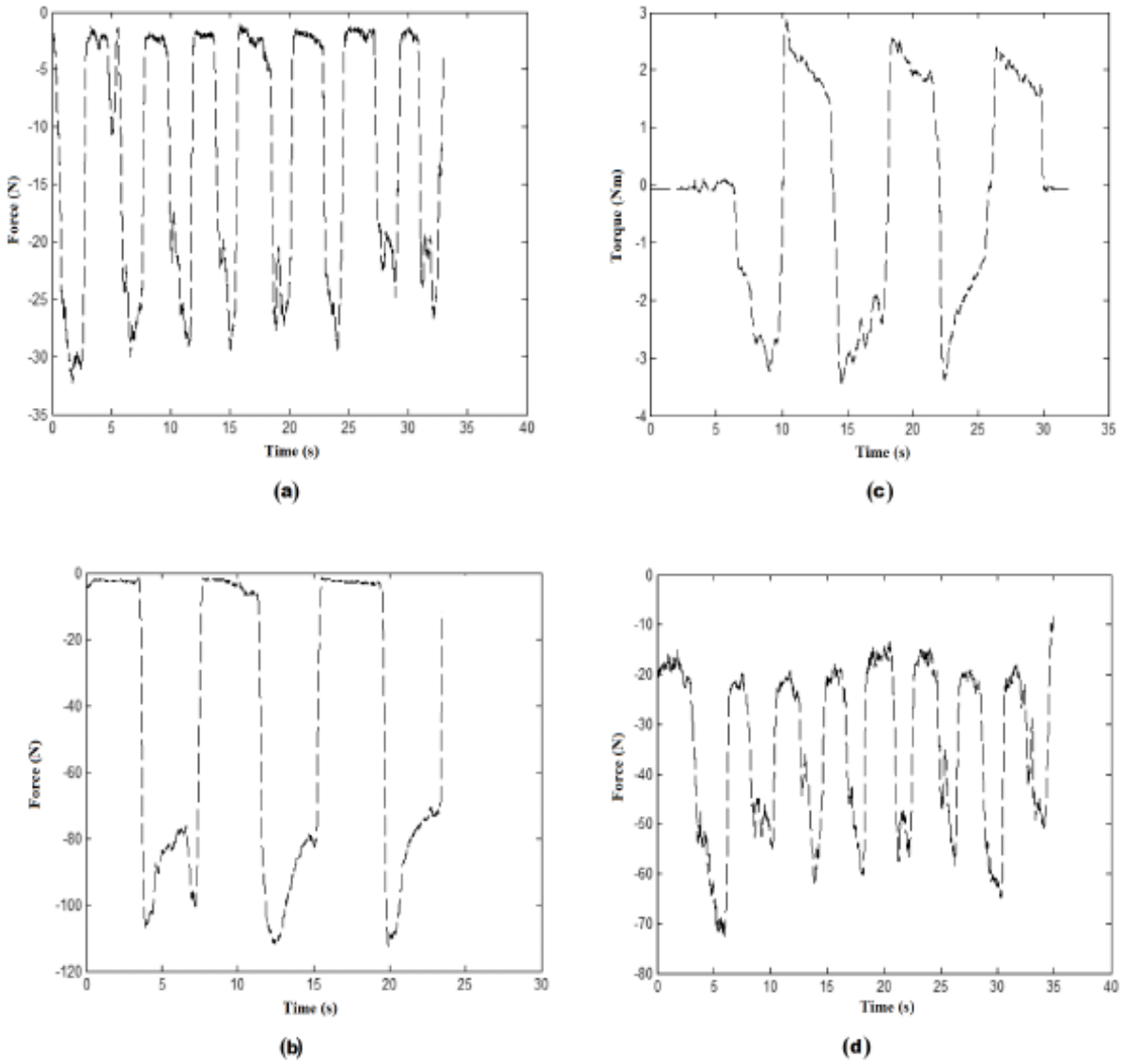

Figure 5.6: Forces and torque representing predefined protocols E, FC, FD and FE. (a) Protocol E, (b) Protocol FC, (c) Protocol FD and (d) Protocol FE.

Table 5.3: Class Definition

Class number	Class definition
1	Rest
2	Pronation arm position: grasp
3	Pronation arm position: radial deviation
4	Pronation arm position: ulnar deviation
5	Pronation arm position: finger pinching - index finger
6	Pronation arm position: finger pinching - middle finger
7	Pronation arm position: finger pinching - ring finger
8	Pronation arm position: finger pinching - little finger
9	Supination arm position: grasp
10	Supination arm position: radial deviation
11	Supination arm position: ulnar deviation
12	Supination arm position: finger pinching - index finger
13	Supination arm position: finger pinching - middle finger
14	Supination arm position: finger pinching - ring finger
15	Supination arm position: finger pinching - little finger

5.5. Results and discussion

The optimal values for the parameters *c* and γ were selected according to the highest value of the cross validation accuracy for each participant. Table 5.4 presents the selected *c* and γ parameters for each of the twelve seniors (denoted with capital letters A-Q in Table 5.4) who participated in this study. Each pair of *c* and γ parameters was used to build a model for classifying the hand gestures of the participant. Results of the classification accuracies for the 12 seniors are presented in Table 5.5. An average accuracy of 90.62% was observed.

The accuracy reached over 95% in the case of the senior Q and less than 85% in the case of the senior L (see Table 5.5). The senior Q controlled the hand functions well, which resulted in an accurate separation between patterns. As an illustrative example, the torque output recorded for the senior Q is shown in Figure 5.7(a). It is clear from this figure that the senior Q was executing the protocol FD (three repetitions of alternating radial and ulnar deviation). On the other hand, the senior L controlled hand functions poorly, which resulted in small separation between patterns. The torque output recorded for the senior L is shown in Figure 5.7(b); it is clear that this senior was not able to correctly follow protocol FD. It should be noted that, although the classification accuracy was smaller for the senior L (see Tables 5.5), it was still acceptable (above 83%).

Table 5.4: The senior cross validation accuracy and model parameters *c* and γ

Senior	*c* and γ	Cross validation accuracy (%)
A	10, 1.2	99.17
B	10, 1.5	97.92
C	10, 0.6	90.42
D	10, 0.8	91.67
I	10, 0.4	90.42
K	10, 0.6	96.67
L	10, 0.4	88.75
M	10, 0.5	99.17
N	10, 0.6	98.33
O	10, 0.4	99.58
P	10, 0.2	95.42
Q	10, 2.4	97.92

Table 5.5: The senior pattern recognition accuracy

Senior	Accuracy percentage (%)	Maximum force (N)	Maximum torque (Nm)
A	91.67	1.79	4.13
B	91.67	2.53	7.03
C	91.67	1.90	5.55
D	87.50	8.84	10.05
I	91.67	1.05	2.14
K	91.67	3.58	7.45
L	83.33	2.12	6.91
M	91.67	3.00	6.45
N	87.50	0.97	1.92
O	91.67	7.01	8.75
P	91.67	1.67	3.58
Q	95.83	2.84	7.10

The system was therefore able to accurately classify the action of the seniors' hand with minimum misclassification, which occurred mainly for finger pinching. Figure 5.8 shows, for example, sEMG signals extracted from ECR, ED, PL and FCU muscles of senior A (Figures 5.8(a)-(d)), the "predicted classes" identified by our classification system (Figure 5.8(e)) and the "actual classes" corresponding to the different protocols

(Figure 5.8(f)). It can be seen that misclassification occurred for consecutive classes related to the finger pinching (see highlighted boxes in Figure 5.8(e)). Specifically, class 7 (ring finger pinching in pronation position) was confused with class 6 (middle finger pinching in pronation position) and class 14 (ring finger pinching in supination position) was confused with class 13 (middle finger pinching in supination position) (see Table 5.3). It should be noted that this misclassification, which probably resulted by a co-contraction of the forearm muscles, is believed to be acceptable for future potential devices assisting finger movements, as generally middle, ring and little fingers have synergistic patterns during functional grasping [85].

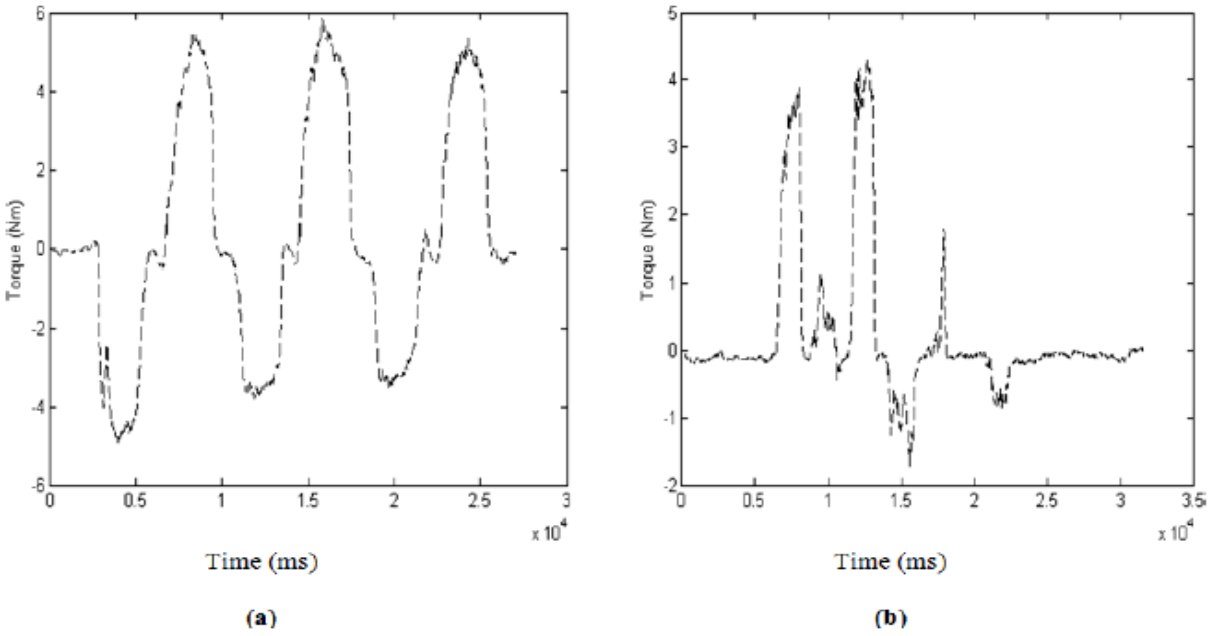

Figure 5.7: The output recorded by the torque sensor for seniors. (a) Senior Q following the protocol FD correctly and (b) Senior L following the protocol FD incorrectly.

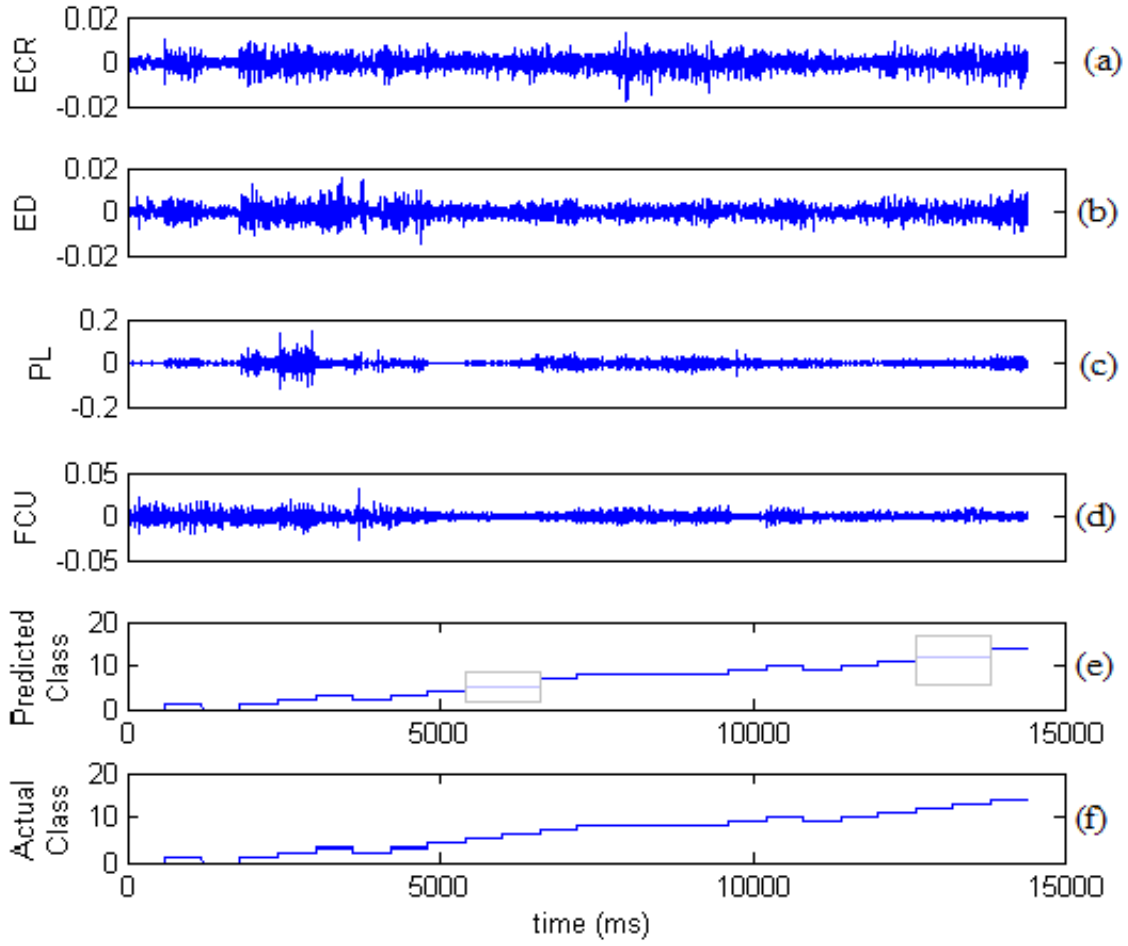

Figure 5.8: System performance. (a) ECR muscle activation, (b) ED muscle activation, (c) PL muscle activation, (d) FCU muscle activation, (e) Predicted class by the system, (f) Actual class.

Table 5.5 also reports the maximum force and the maximum torque each senior was able to exert. The average maximum force was 3.11N and the average maximum torque was 5.92 Nm. No clear relationship was identified between classification accuracy and maximum force or maximum torque exerted by the participants. For example, participants D and N had equal classification accuracy but their maximum force and torque were respectively the highest and the smallest of the entire group of seniors.

Table 5.6 and Table 5.7 respectively present the selected c and γ parameters and the corresponding classification accuracies for the group of young participants. An average classification accuracy of 97.6% was obtained. Table 5.7 also reports the maximum force and maximum torque each young participant was able to exert. The

average maximum force was 4.20N and the average maximum torque was 3.37 Nm. In this case, data suggests a linear relationship between classification accuracy and maximum force and maximum torque, as shown in Figure 5.9. It should however be noted that the number of young participants participating in this study was limited to 7.

A comparison between results obtained for seniors and the young participants shows that while maximum force decreased of about 26%, classification accuracy decreased of only 7% with age. Although there are major physical changes occurring in humans while ageing [80], successful sEMG classification is therefore possible in seniors.

Table 5.6: The young participant cross validation accuracy and model parameters c, γ

Young participants	c and γ	Cross validation accuracy (%)
Y_R	15, 0.9	99.17
Y_S	10, 0.9	94.58
Y_T	10, 1.1	93.33
Y_U	10, 0.2	96.67
Y_V	10, 0.5	97.50
Y_W	10, 0.3	93.75
Y_X	70, 0.2	99.58

Table 5.7: The young participant pattern recognition accuracy

Young participant	Accuracy percentage (%)	Maximum force (N)	Maximum torque (Nm)
Y_R	91.67	1.86	0.38
Y_S	100.00	5.91	2.65
Y_T	100.00	5.27	5.89
Y_U	95.83	4.44	3.57
Y_V	100.00	4.09	3.82
Y_W	95.83	1.88	2.61
Y_X	100.00	5.90	4.69

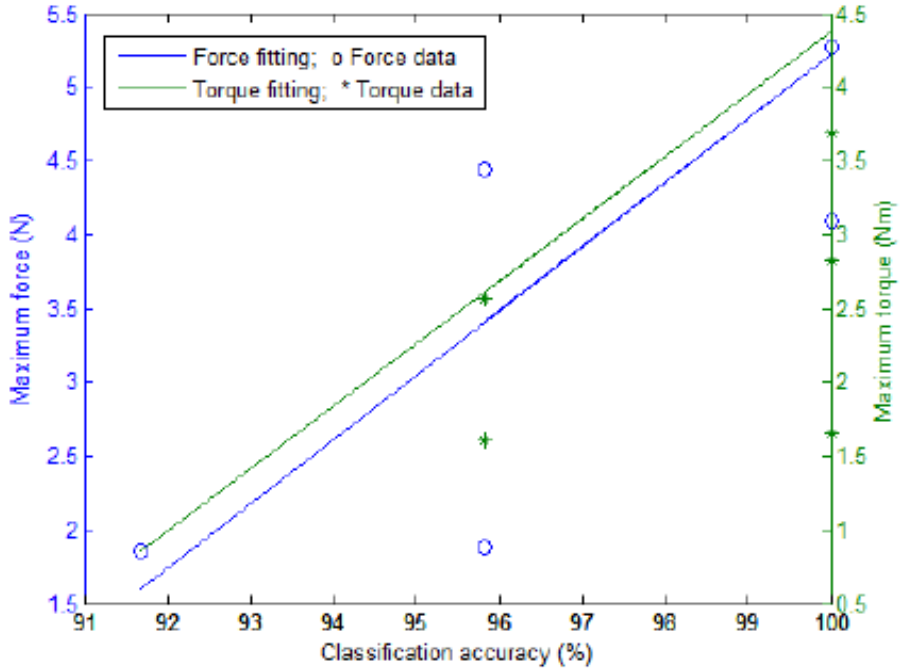

Figure 5.9: The relationship between the maximum force/torque and the classification accuracy.

5.6. Conclusions

This chapter was an attempt to validate the use of the SVM classification approach to be used later on the BCI method. The possibility of associating forearm sEMG patterns to different hand postures was investigated. Results support the hypothesis that successful pattern recognition can be performed to distinguish different hand gestures in vital activities of daily living.

The identified classes in this study were grasping, radial/ulnar deviation and four different finger pinching in both pronation and supination positions of the arm. The use of only four sEMG channels demonstrated to be suitable for classifying the fifteen different hand gestures considered in this study. In fact, the implemented pattern recognition strategy was able to identify the different hand gestures with average accuracy greater than 90%.

Chapter 6. Experimental Procedure

6.1. Introduction

This chapter provides a brief description of experimental procedure including signal acquisition and analysis for different motor imageries. The EEG data collected from each experiment contained a mixture of different mental states. Two mental states were utilized to address objective 1.1 and objective 1.2. Three mental states were utilized to address objective 2.

6.2. Signal Acquisition

There are several ways to acquire signals from the brain, all falling into two main categories: invasive and non-invasive techniques. Invasive BCIs use activity recorded by brain implanted micro-electrodes, whereas non-invasive BCIs use brain signals recorded from outside the body boundaries. Non-invasive technique is adopted in this study.

6.3. EEG Recording

Twelve able-bodied individuals were recruited for the experiment. Participants gave a written informed consent before participating in the experiment. Each individual was seated comfortably in front of a computer monitor and the computer provided a simple Graphical User Interface that displays commands or cues to the participant. A 32-channel EGI's Geodesic sensor net [86] was applied on the participant's head. The locations of all the electrodes are shown in Figure 6.1. The letters and numbers used in these labels were described in chapter 2.

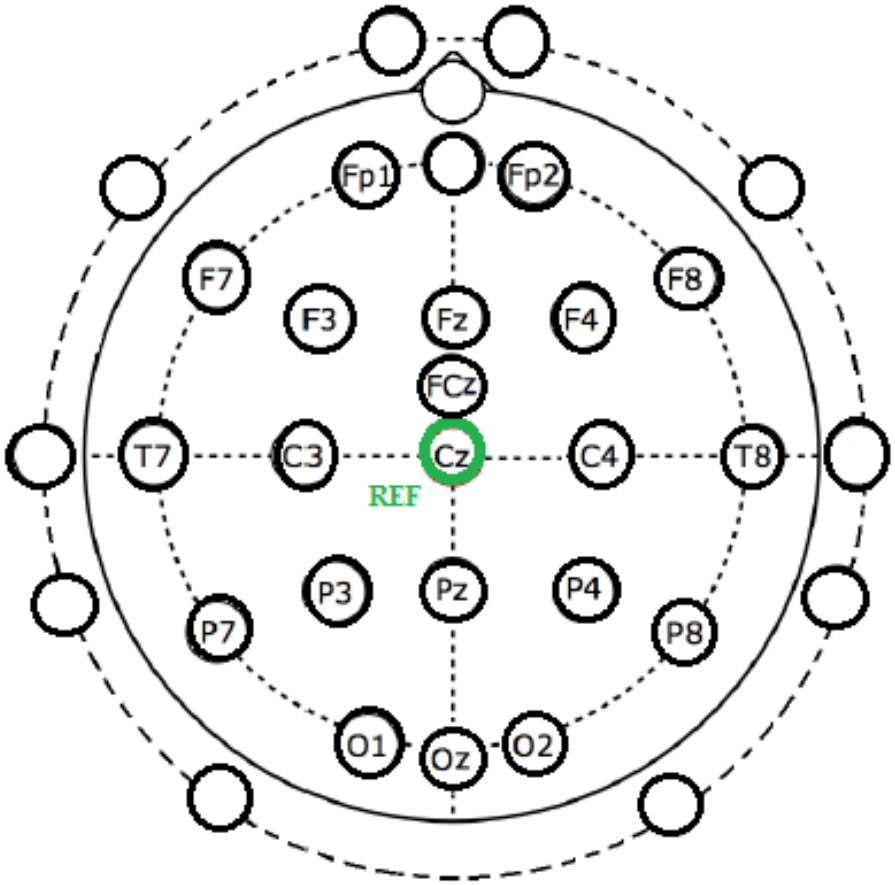

Figure 6.1: The EEG electrode positions

The labeled electrodes were those employed for the proposed BCI system. The remaining unlabeled electrodes, on the other hand, were not considered in this study because they were very close to sources that generate muscle activities or artifacts. All these electrodes were referred to the vertex (Cz position in Figure 6.1) of the participant. This reference was selected as it is very commonly used [87], often the one adopted by equipment designed to record EEG signals, including the one we used (EGI system) [88, 89], and is the same that was used in PS. The EEG signals were amplified and sampled at 1000 Hz using a Geodesic Net Amps 400 series amplifier [90]. Throughout the experiment, the electrode impedance was maintained below 50 k.

6.4. Experimental Procedure

Each experiment for each participant lasted for approximately 1.5 hours. The experiment consisted of four sessions. Each session lasted 12 minutes. The participant was asked to perform different repetitive tasks according to the visual cues displayed on the computer monitor. Three different visual cues were presented to the participant, as illustrated in Figure 6.2. They are listed as follows:

• Rest (REST): rest and relax [Figure 6.2 A]

• Motor imagery of grasp (MI-GRASP): imagine opening and closing all the fingers to grab an object [Figure 6.2 B]

• Motor imagery of elbow flexion and extension (MI-ELBOW): imagine moving the forearm up and down [Figure 6.2 C]

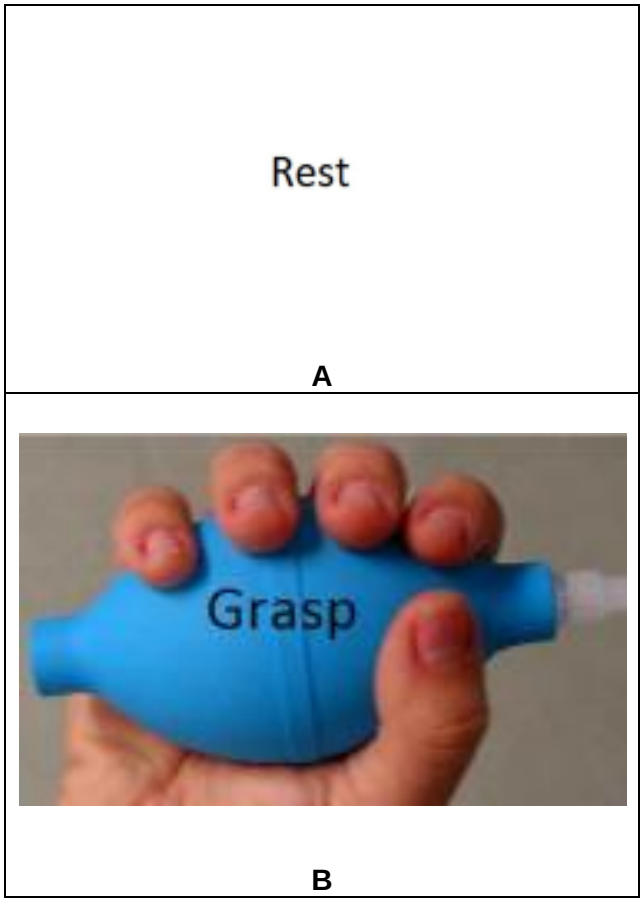

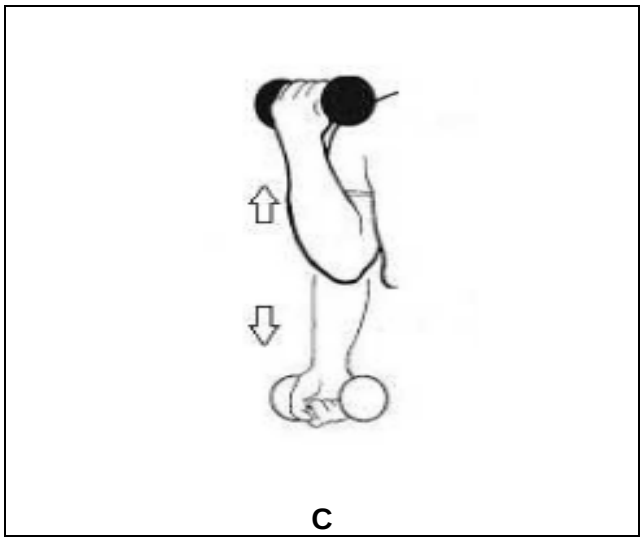

Figure 6.2: Visual cues presented during the experiments. (A) Rest: rest and relax. (B) Motor imagery of grasp: imagine opening and closing all the fingers to grab an object. (C) Motor imagery of elbow flexion and extension: imagine moving the forearm up and down

Each session consisted of 20 trials for each tasks. Each trial lasted from 8 to 10 s (see Figure 6.3). Each visual cue was randomly selected and displayed on the screen for 3 s, indicating which task to perform. The participant was asked to perform each designated task for 3 s, followed by 5 to 7 s of rest. Throughout the experiment, the participant could take a break whenever needed.

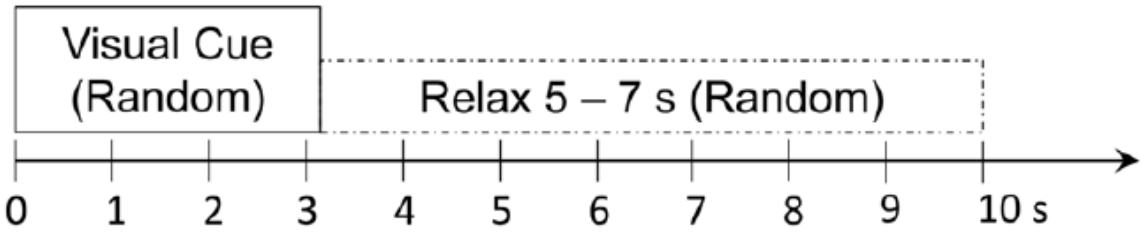

Figure 6.3: Experimental paradigm. At 0 s, a visual cue is randomly selected and presented. After 3 s, a blank screen appears for 5 −7 s before another visual cue is presented. During this period of time, the participant is requested to rest.

To collect data for both objectives 1 and 2, the EEG data collected from each experiment contained a mixture of three different mental states: REST, MI-GRASP, and MI-ELBOW. First the binary classifications of the following combinations were performed (objective 1):

1. REST versus MI-GRASP

2. REST versus MI-ELBOW

Then, the classifications of the following three classes were performed (objective 2):

1. REST versus MI-GRASP versus MI-ELBOW

6.5. Data Preprocessing

The EEG data were down sampled to 250 Hz and then band-pass filtered to the 6–35 Hz frequency band. This frequency band encompasses the beta and mu rhythms of EEG signal which desynchronizes during motor movement imagery [91]. The band power changes of the beta and mu rhythms were successfully used in BCI systems for classifying EEG signals related to motor movement imagery [92–94]. In addition, ocular artifacts caused by the low frequency components of the EEG data were minimized by band-pass filtering the data.

6.6. CSP, FBCSP and Band Power

Common Spatial Patterns (CSP) [93], Filter-Bank Common Spatial Patterns (FBCSP) [95] and Logarithmic Band Power [12] feature extraction methods, which are widely used in BCI research, were employed in this study. CSP, FBCSP and band power methods [12, 96-97] were used in order to compare their performances with the performance obtained using the proposed classification scheme.

An open-source MATLAB toolbox, BCILAB [98], was utilized to process the acquired EEG data. The EEG data was pre-processed as previously mentioned in the pre-processing section. Following PS [23], EEG data was divided to epochs from 1 to 3 s after the cue was given to the participant. CSP [93], FBCSP [95], and band power [12] methods were applied to these EEG epochs. For each EEG epoch, 6, 18, and 20 features were respectively obtained from CSP [93], FBCSP [95], and band power [12]

methods. For the FBCSP method, as in PS [23], the signal was further broken down into 7–15 Hz, 15–25 Hz, and 25–30 Hz frequency sub-bands.

CSP has been widely used in BCI research to extract features from EEG signals. This algorithm can effectively extract discriminatory information from two classes of EEG signals [93]. The algorithm finds the directions where the EEG signals should be projected onto so that the differences between any two classes of EEG signals are maximized (i.e. the variance of one class is maximized while at the same time, the variance of the other class is minimized) [92]. These directions are provided by a weight matrix in which its rows give the weights of the EEG channels.

Here, the formulation of the CSP algorithm for a 2-class problem is described. This same formulation of the 2-class CSP algorithm was also used when classifying the three classes of EEG signals. More specifically, for a 3-class problem, three different binary classifiers were trained and a voting scheme was employed to determine the class label.

Given two classes of EEG signals: Class 1 and Class 2, the CSP algorithm finds a spatial filter such that the signals can be projected into a 1-dimensional space where one class of signals is maximally scattered and the other is minimally scattered. High variance of the signals indicates strong rhythms whereas low variance indicates attenuated rhythms [92]. Let S = {S_1, S_2 . . ., S_M} where $S_i \in R^{N_c \times N}$ denotes the filtered *i*-th trial EEG signal, *M* the number of EEG trials, N_c the number of EEG channels, and *N* the number of samples in the signal. The optimization problem is expressed as:

$$\min_{w} \sum_{i \in C_1} \text{var}\,(W^T S_i) \tag{9}$$

$$\text{s.t.} \sum_{i=1}^{2M} \text{var}(W^T S_i) = 1 \tag{10}$$

where C_1 represents all Class 1 EEG trials, $w \in R^{N_c}$ is the unknown weight vector of the spatial filter and var is the variance. In this study, the CSP features selected for classification were the log-variance of the EEG signals projected using six different spatial filters. These spatial filters were a) the three most important spatial filters that

explain the largest variance of Class 1 and the smallest variance of Class 2 and b) the three most important spatial filters that explain the largest variance of Class 2 and the smallest variance of Class 1.

FBCSP is an extension of the CSP algorithm [95]. First, a filter bank is used to bandpass filter the EEG signals. Then, for each filtered EEG band, spatial filters are found using the CSP algorithm discussed earlier. The FBCSP features selected for classification were the log-variance of each of the filtered EEG band projected using six different spatial filters.

The third method logarithmic band power is a simpler method. The features used for classification were the log-variance of the band-pass filtered EEG signals from every channel.

6.7. Topographical Analysis for Different Motor Imageries

Figure 6.4 illustrates the topographical distribution on the scalp of the difference between rest and imaginary grasp movements. The R^2 values for frequency bands ranging from 8 to 24 Hz at each electrode locations were computed for all participants. R^2 measures the difference between two classes, i.e., the proportion of the single-trial variance that is due to the task [34]. The topographical map of one of the participants (P06) is shown in Figure 6.4. The topographical map demonstrates prominent scalp difference between rest and imaginary grasp movements. Large R^2 values are observed at electrode locations near the contra-lateral motor cortex area. Such prominent differences occur as a result of the ERD of the beta and mu rhythms when motor imagery tasks are executed.

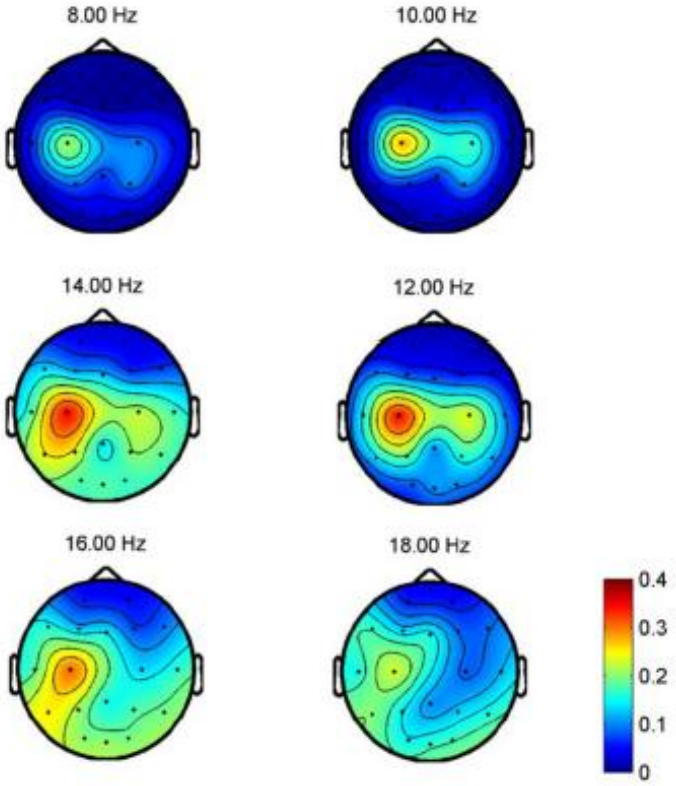

Figure 6.4: R^2 values for REST versus MI-GRASP for participant P06. R^2 measures the difference between REST and MI-GRASP classes. The R^2 values for frequency bands ranging from 8 to 24 Hz at each electrode locations were computed for all participants. Large R^2 values were observed at electrode locations near the contralateral motor cortex area.

Topographical analysis could highlight the difference that could be observed in different areas of the brain for each participant during imagery movements. Such information could be useful in building a customized model for each participant. The topographical distribution on the scalp for these motor imagery tasks was measured by R^2 values. The topographical difference was participant-specific and no consistent patterns could be observed. An example of the results obtained from the topographical analysis to study the EEG signals for MI-GRASP and MI-ELBOW for participants P06 and P07 is presented in Figures 6.5 A and B respectively. Larger difference was observed in the contra-lateral of the motor cortex in participant P06 for the case of MI-GRASP versus MI-ELBOW. However, in participants P07, larger difference was observed in the ipsi-lateral of the motor cortex for the case of MI-GRASP versus MI-ELBOW.

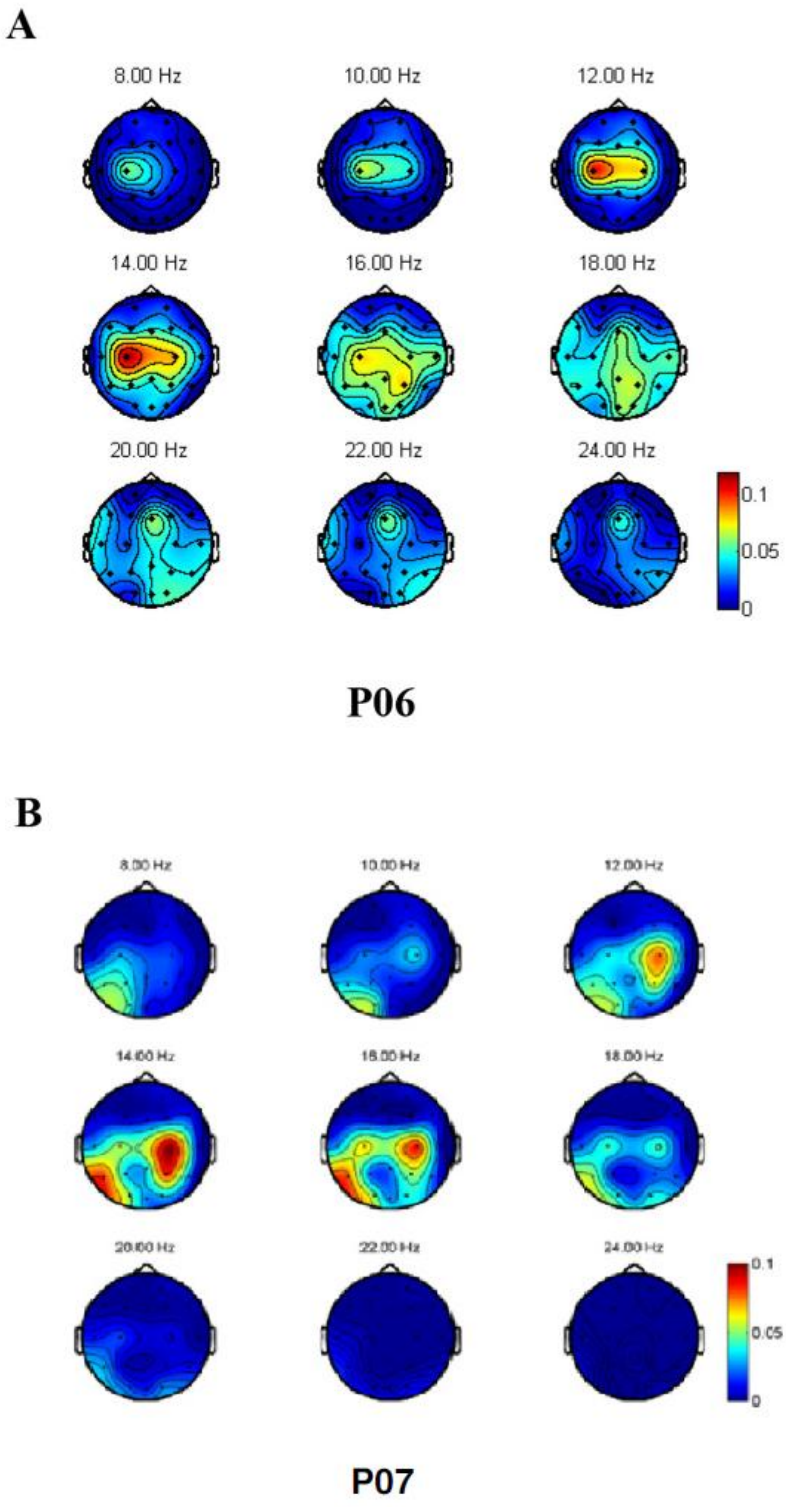

Figure 6.5: R^2 values when different MI tasks were performed. (A) MI-GRASP versus MI-ELBOW for participant P06. (B) MI-GRASP versus MI-ELBOW for participant P07.

6.8. Conclusion

The experimental setup, the data acquisition stage and the preprocessing stage were explained. Widely used methods, CSP, FBCSP and Band power were also briefly described. The next chapters present the performance of the proposed method, which are compared with the performance of these well-known methods.

Chapter 7. Identifying Rest State versus Upper Extremity Imagery Motor Movement

7.1. Introduction

This chapter presents the obtained optimal kernel parameters for binary classification of REST versus MI-GRASP and REST versus MI-ELBOW. Objective 1.1 and objective 1.2 are addressed in this chapter and the classification accuracies obtained for each participant are reported. The content of this chapter was slightly modified from what first appeared in print in:

Tavakolan M, Yong X-Y, Zhang, X, and Menon C (2016) Classification Scheme for Arm Motor Imagery, Journal of Medical and Biological Engineering. Vol 36, No.1, pp 12-21.

7.2. REST versus MI-GRASP, REST versus MI-ELBOW Classification Models

In order to obtain the specific binary classification model for each participant, the optimal values for the kernel parameters were selected according to the highest value of the cross-validation accuracy. The obtained optimal kernel parameters were then used to build a model for binary classification of rest versus imagined arm movements. Figure 7.1 shows the obtained results for the kernel parameters for binary classification of MI-GRASP and MI-ELBOW versus REST for a single participant. As shown, the highest cross-validation accuracy occurred in the interval (0, 3) for γ and (0, 100) for *c*. These intervals were selected for the identification of the optimal kernel parameters for all participants.

The obtained optimal kernel parameters for binary classification of REST versus MI-GRASP and REST versus MI-ELBOW are respectively presented in Tables 7.1 and Table 7.2 for each of the twelve participants (denoted as P01-P12). These selected parameters were then used to build the optimal pattern recognition model for each individual. The reported classification accuracy for each participant is the percentage of data which were correctly classified. The pattern recognition accuracies obtained using the optimal models of the proposed method are presented in the following tables. The

obtained classification accuracy of REST versus MI-GRASP is presented in Table 7.1 and the obtained classification accuracy of REST versus MI-ELBOW is presented in Table 7.2.

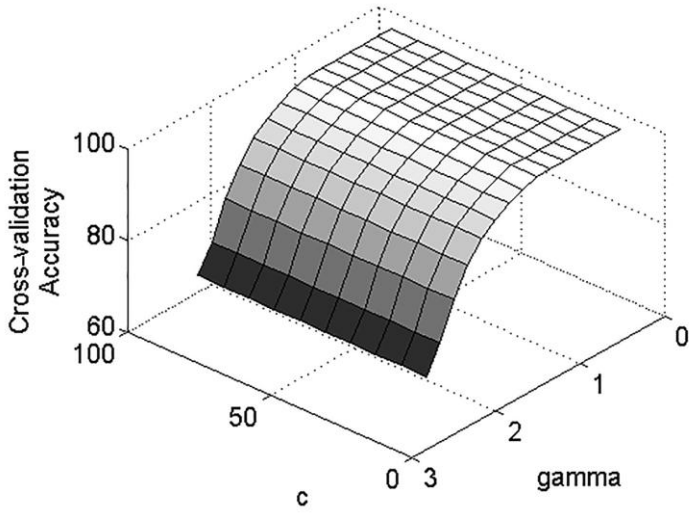

A

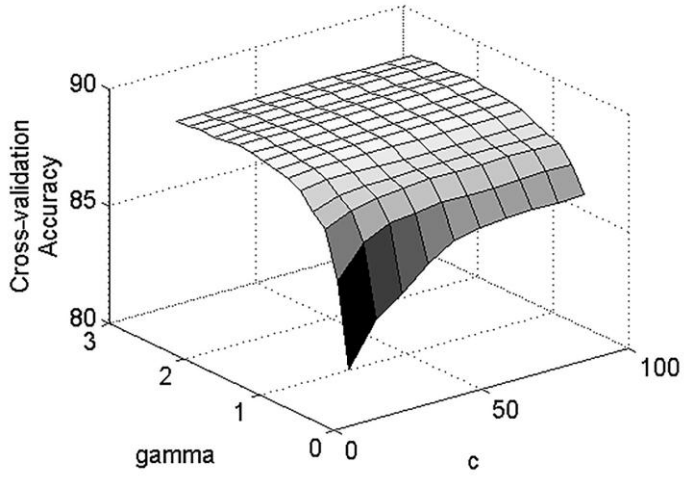

B

Figure 7.1: Cross-validation accuracies based on *c* and γ parameters. (A) REST versus MI-GRASP. (B) REST versus MI-ELBOW.

Table 7.1: Binary classification result – REST versus MI-GRASP

Participants	Optimal parameters *c* and γ REST versus MI-GRASP	Classification accuracy REST versus MI-GRASP
Participant P01	10, 0.2	100
Participant P02	10, 0.2	100
Participant P03	10, 2.3	83
Participant P04	10, 1.9	88.5
Participant P05	15, 1.7	87.8
Participant P06	15, 1.1	86.7
Participant P07	10, 1.4	87.9
Participant P08	10, 1.9	87.4
Participant P09	10, 1.6	94.4
Participant P10	70, 1	98.5
Participant P11	90, 1	95.9
Participant P12	10, 2.5	90.8

Table 7.2: Binary classification result – REST versus MI-ELBOW

Participants	Optimal parameters *c* and γ REST versus MI-ELBOW	Classification accuracy REST versus MI-ELBOW
Participant P01	10, 1.7	89.3
Participant P02	90, 0.4	89.6
Participant P03	10, 1.6	83.6
Participant P04	10, 1.5	89.4
Participant P05	10, 2.2	87
Participant P06	15, 1.1	86.2
Participant P07	10, 2	89.9
Participant P08	10, 2.3	87
Participant P09	10, 2	95.2
Participant P10	35, 2.3	97.7
Participant P11	30, 2.1	94.9
Participant P12	10, 1.4	90.3

7.3. Kernel Parameters

Optimizing the kernel parameters was the key factor in improving the performance of the proposed method. It was demonstrated that on average the performance of the RBF kernel function with optimal parameters was higher compared to that with non-optimal parameters. Figure 7.2 compares the obtained performances using optimal and non-optimal parameters for each individual. As shown, the pattern recognition accuracy of the RBF kernel function with optimal parameters was higher compared to that of the RBF kernel function with non-optimal parameters for all participants. On average, the pattern recognition rate increased by more than 9% for identifying MI-GRASP and MI-ELBOW patterns versus the REST pattern when the optimal parameters were used (see Figure 7.3).

The overall results obtained for the proposed method is acceptable and promising. 100% accuracy was obtained for participants P01 and P02 for binary classification of REST versus MI-GRASP. Accuracies of over 90% were obtained for participants P09, P10, P11, and P12 for both cases of REST versus MI-GRASP and REST versus MI-ELBOW.

With the use of the RBF kernel SVM, the postures associated to the imaginary tasks were predicted with an average overall accuracy of 91.8% and standard deviation of 5.8% for the case of REST versus MI-GRASP and an average overall accuracy of 90% and standard deviation of 4.1% for the case of REST versus MI-ELBOW.

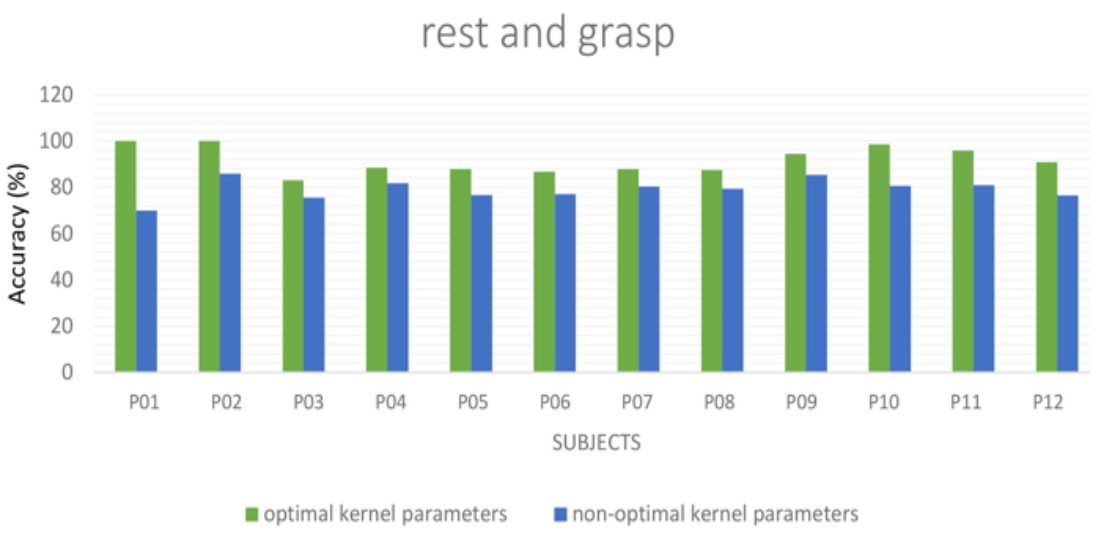

A

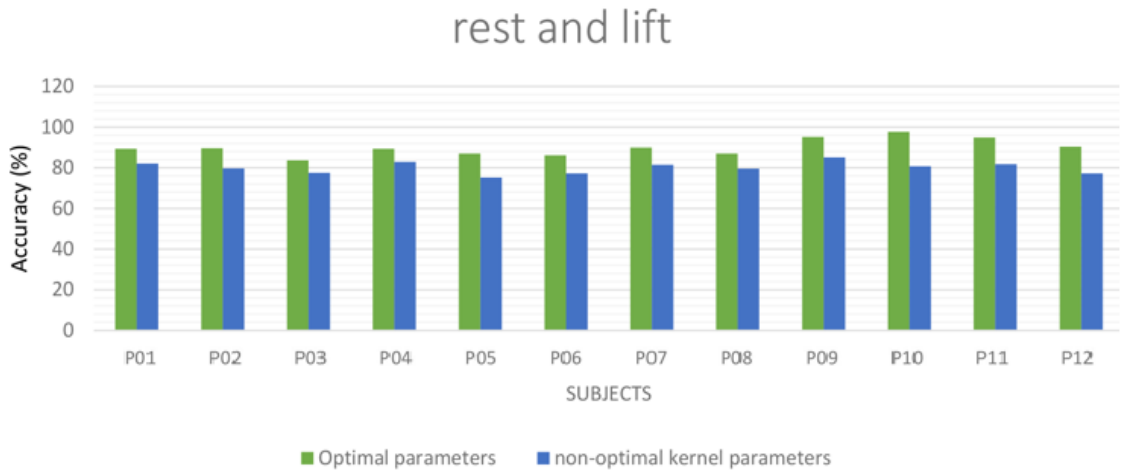

B

Figure 7.2: Classification accuracies of proposed method using optimal and non-optimal parameters for each individual. (A) REST versus MI-GRASP. (B) REST versus MI-ELBOW.

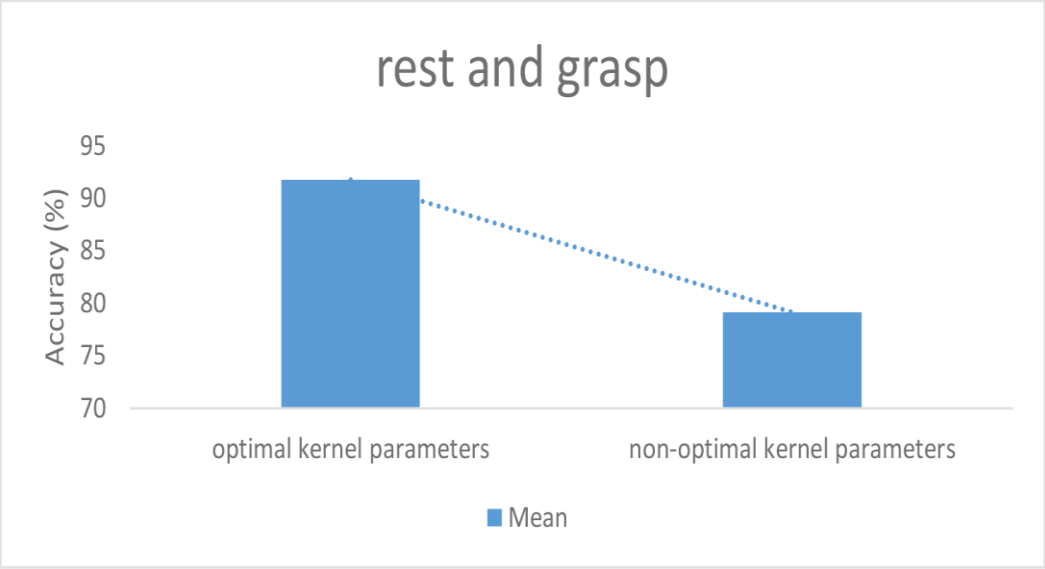

A

B

Figure 7.3: Average classification accuracies of proposed method using RBF kernel for optimal and non-optimal parameters. (A) REST versus MI-GRASP. (B) REST versus MI-ELBOW.

7.4. Conclusion

The results of the implementation of the method for both two investigations were presented in this chapter. For each investigation, the results obtained for different parameters used for selecting optimal parameters were plotted, followed by the classification accuracies, which were shown for individual subjects based on optimal and non-optimal parameters. The next chapter discusses the results in relation to the purpose of the research for identifying multi-classes of motor imageries.

Chapter 8. Recognition Performance of the Multi-Class Classification Model for the Upper Extremity Imagery Motor Movement

8.1. Introduction

This chapter presents the obtained optimal kernel parameters for multi-class classification of REST versus MI-GRASP versus MI-ELBOW. Objective 2 is addressed in this chapter and the classification accuracies obtained for each participant are reported. The content of this chapter was slightly modified from what first appeared in print in:

Tavakolan, M, Frehlick, Z, Yong X-Y, Menon, C (2017) Classifying three imaginary states of the same upper extremity using time-domain feature, PLoS ONE, Vol.12, No3, 18pp.

8.2. REST versus MI-GRASP versus MI-ELBOW Classification Model

The goal was to build the specific multi-class classification model for each participant for classifying REST versus MI-GRASP versus MI-ELBOW. The performance obtained from different model parameters for participant P01 is presented in Figure 8.1 A. The highest cross-validation accuracy occurred in the interval (0, 3) for γ and (0, 100) for *c*. Figure 8.1 B-L also shows that the highest cross-validation accuracy occurred in the same interval for other participants (participants P02 - P12). These intervals were selected for the identification of the optimal range of the SVM parameters for all the participants.

A

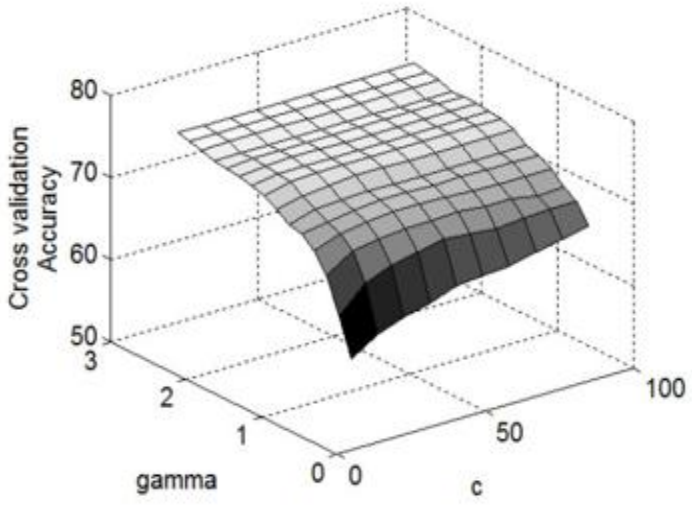
Cross validation Accuracy
80
70
60
50
3
2
1
0
gamma
0
50
100
c

P01

B

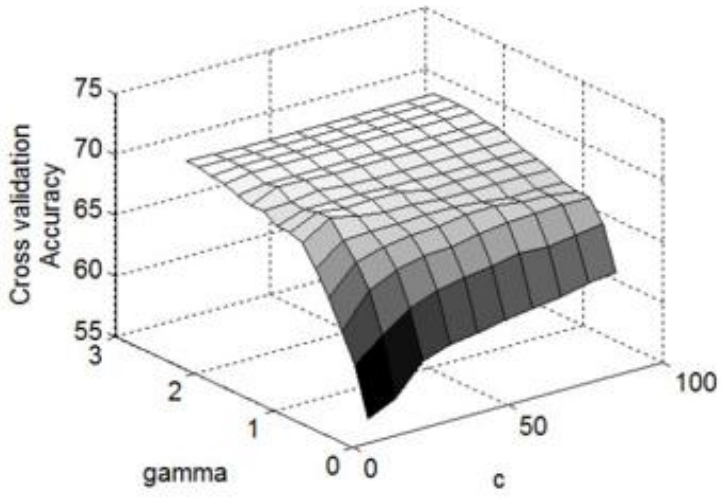
Cross validation Accuracy
75
70
65
60
55
3
2
1
0
gamma
0
50
100
c

P02

C

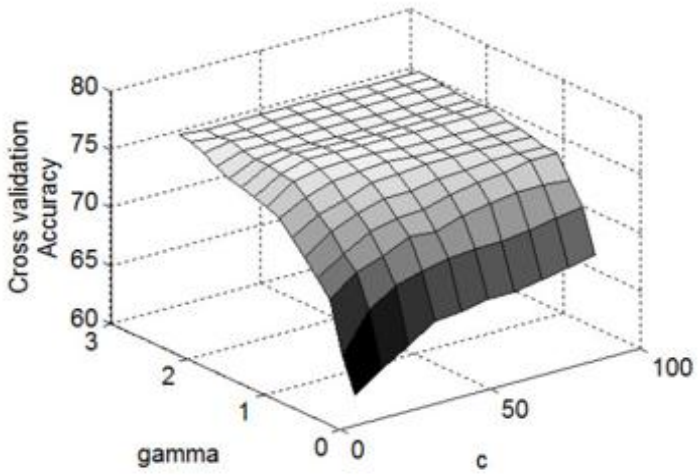
Cross validation Accuracy
80
75
70
65
60
3
2
1
0
gamma
0
50
100
c

P03

D

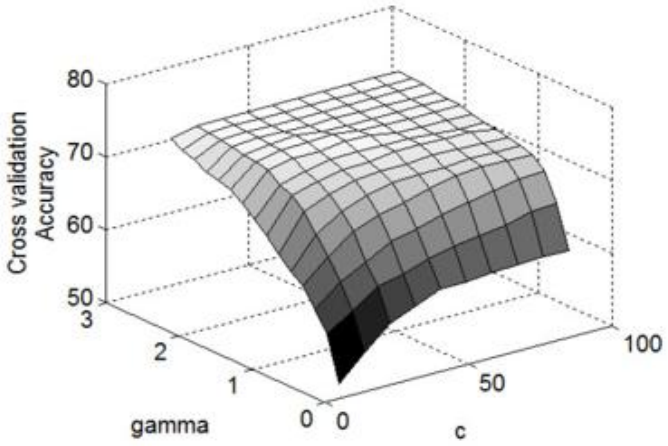
Cross validation Accuracy
80
70
60
50
3
2
1
0
gamma
0
50
100
c

P04

E

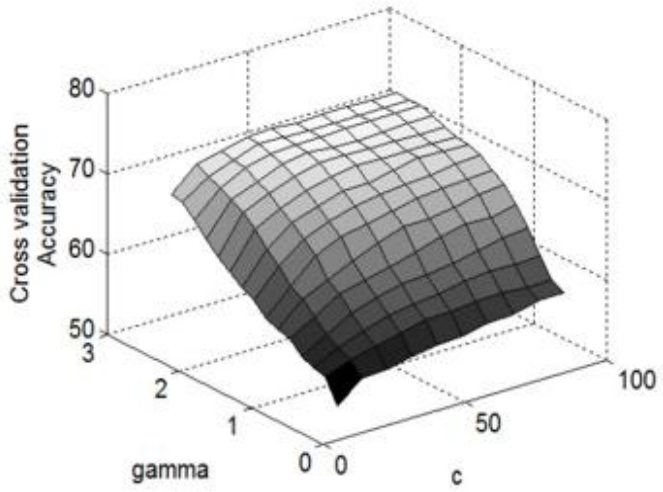
Cross validation Accuracy
80
70
60
50
3
2
1
0
gamma
0
50
100
c

P05

F

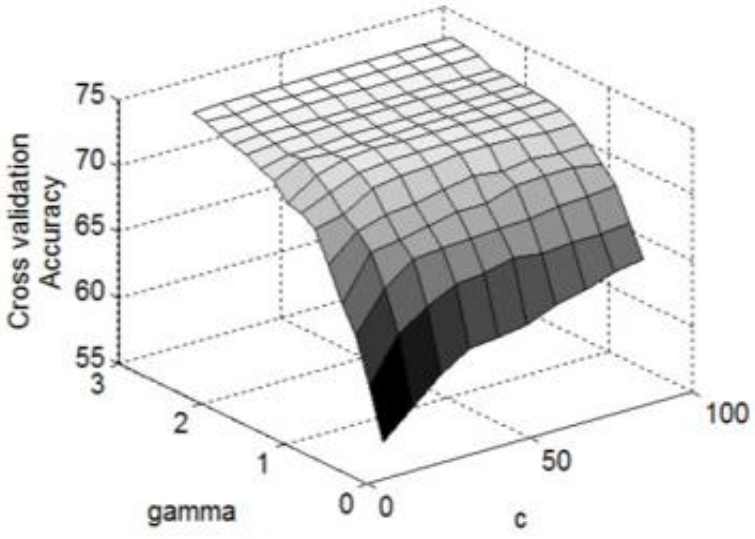
Cross validation Accuracy
75
70
65
60
55
3
2
1
0
gamma
0
50
100
c

P06

G

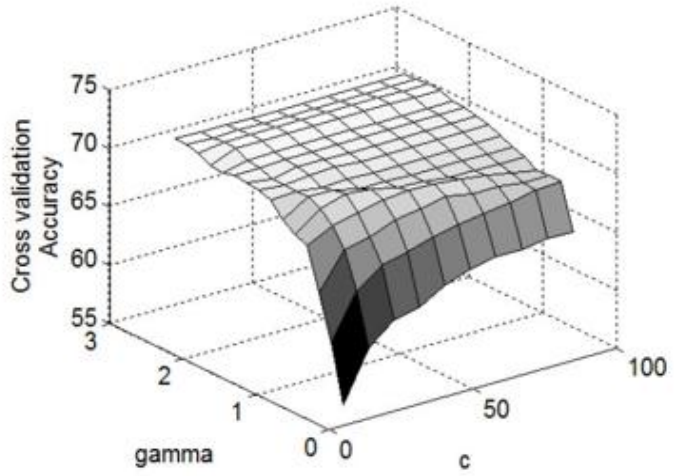
Cross validation Accuracy
75
70
65
60
55
3
2
1
0
gamma
0
50
100
c

P07

H

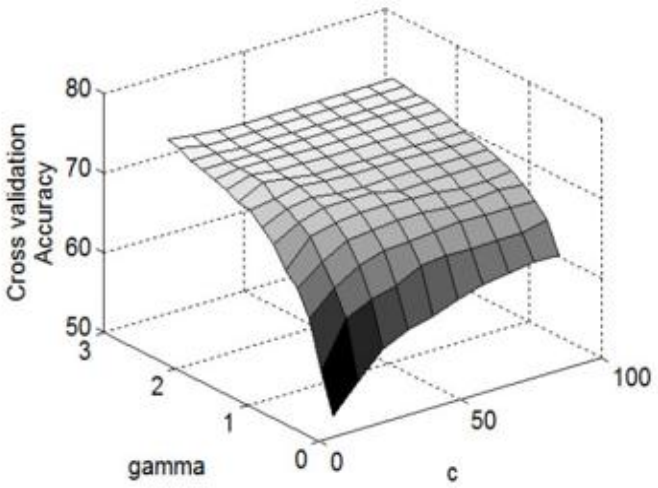
Cross validation Accuracy
80
70
60
50
3
2
1
0
gamma
0
50
100
c

P08

I

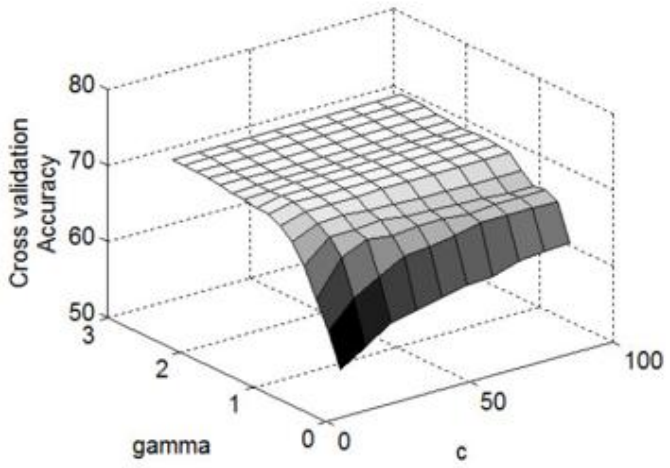
Cross validation Accuracy
80
70
60
50
3
2
1
0
gamma
0
50
100
c

P09

J

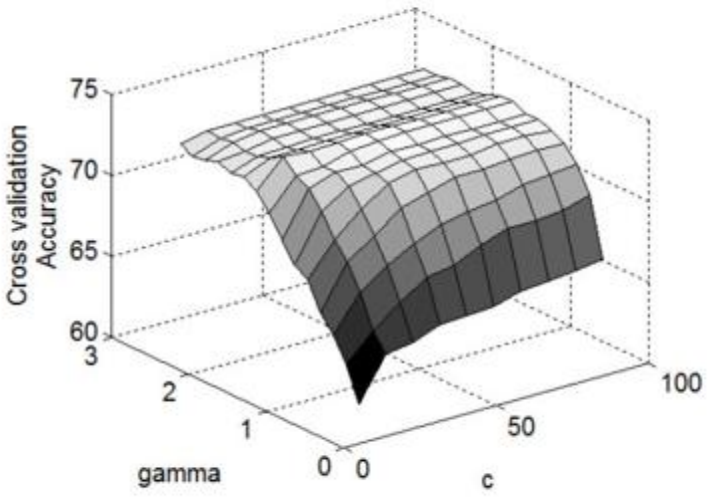
Cross validation Accuracy
75
70
65
60
3
2
1
0
gamma
0
50
100
c

P10

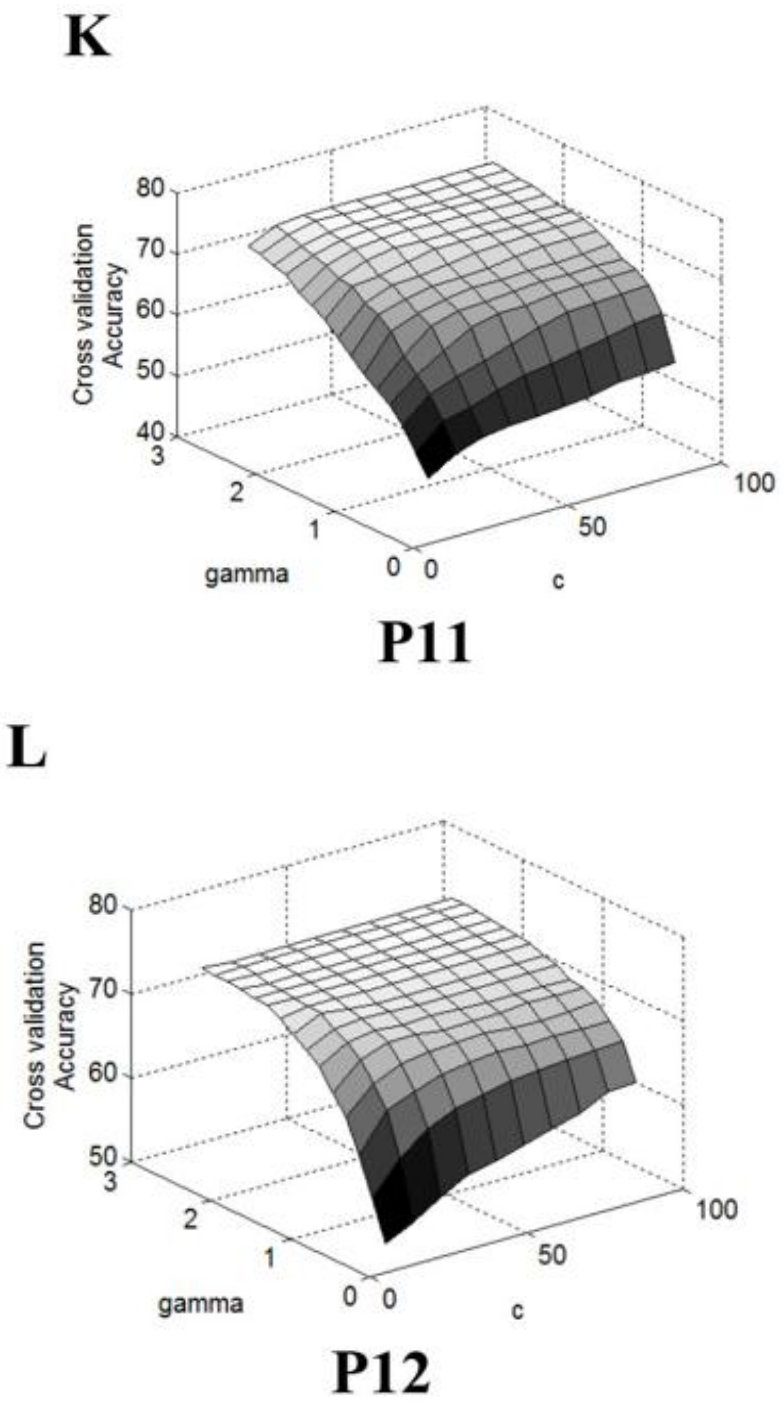

Figure 8.1: Cross validation accuracies of REST versus MI-GRASP versus MI-ELBOW based on *c* and γ parameters. (A) Participant P01. (B) Participant P02. (C) Participant P03. (D) Participant P04. (E) Participant P05. (F) Participant P06. (G) Participant P07. (H) Participant P08. (I) Participant P09. (J) Participant P10. (K) Participant P11. (L) Participant P12.

8.3. Kernel Parameters

Table 8.1 presents the classification accuracy obtained using the selected optimal parameters and other kernel parameters for each participant. Table 8.2 presents the corresponding selected optimal values of *c* and γ for each participant. The proposed method using the selected optimal parameters achieved an average accuracy of 74.2%, which was significantly higher than that obtained using the non-optimal parameters (55.2%). The importance and sensitivity of selecting the optimal SVM parameters is clear. For instance, the proposed method selected *c* = 25 and γ = 2.3 for participant P04, and the classification accuracy achieved was 74.8%. However, if, for example, *c* = 10 and γ = 0.2 were selected, the accuracy dropped to 50.7%; if *c* = 50 and γ = 0.9, the accuracy was 72.1%. The same trend can be observed in other participants when different values for *c* and γ parameters were used.

Similar to the case of binary classification, optimizing the SVM parameters was also found the key to improving the performance of the proposed method for multi-class classification. It was demonstrated that on average, the accuracy of the SVM using RBF kernel function and optimal parameters was higher compared with the accuracy of SVM using RBF kernel function with non-optimal parameters (see Figure 8.2 A). The performance gain was 19% on average. Figure 8.2 B presents in detail the comparison of classification using the optimal and non-optimal parameters for each participant. For all the participants, the classification accuracy of the SVM with optimal parameters was higher than that with non-optimal parameters.

The optimal SVM parameters used in the proposed multi-class classification scheme and the average cross-validation accuracy achieved for each participant using the parameters in the selected interval are presented in Table 8.2. The overall results obtained from the proposed method is encouraging as the accuracies achieved as greater than 70.0% for nine participants in this study.

Table 8.1: Comparison of the performance obtained when different γ and c values of the SVM were used in the proposed method.

Participant	Accuracy	$c,10$ $\gamma,0.2$	$c,20$ $\gamma,0.3$	$c,30$ $\gamma,0.5$	$c,40$ $\gamma,0.7$	$c,50$ $\gamma,0.9$	$c,60$ $\gamma,1.1$	$c,70$ $\gamma,1.3$	$c,80$ $\gamma,1.5$	$c,90$ $\gamma,2.5$
P01	76.8	59.6	65.5	70.7	72.9	73.4	73.9	75.2	75.3	76.7
P02	70.3	56.1	61.0	66.1	68.2	68.5	68.9	69.0	69.3	70.2
P03	77.2	61.7	66.7	71.6	73.9	75.2	75.9	76.3	76.6	76.9
P04	74.8	50.7	57.8	63.5	69.0	72.1	73.1	73.3	73.2	74.6
P05	73.2	52.9	56.7	58.9	62.1	65.0	67.4	69.5	71.2	73.0
P06	75.0	56.9	62.9	68.5	69.7	71.8	73.3	73.6	73.8	75.0
P07	71.9	55.8	63.0	67.9	69.9	69.6	69.9	70.6	70.9	71.6
P08	75.5	51.2	60.5	66.9	69.9	71.1	71.5	72.4	72.5	74.7
P09	72.2	55.0	61.1	68.6	69.6	70.3	71.7	71.4	71.7	72.1
P10	73.9	61.8	65.1	68.5	71.8	73.0	73.3	73.4	73.6	73.0
P11	75.7	48.9	54.8	61.1	67.8	69.6	70.7	72.7	73.4	75.5
P12	74.5	52.1	58.5	66.6	70.0	70.8	72.0	72.3	73.2	74.1
Mean	74.2	55.2	61.1	66.6	69.6	70.9	71.8	72.5	72.9	74

A

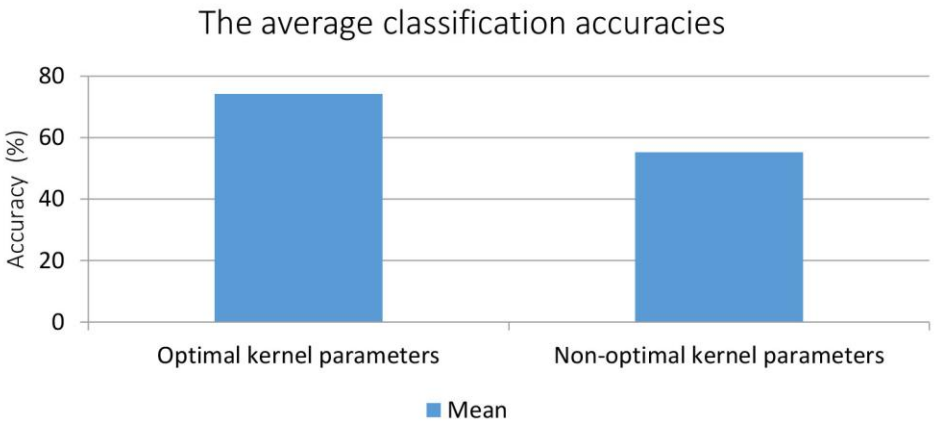

B

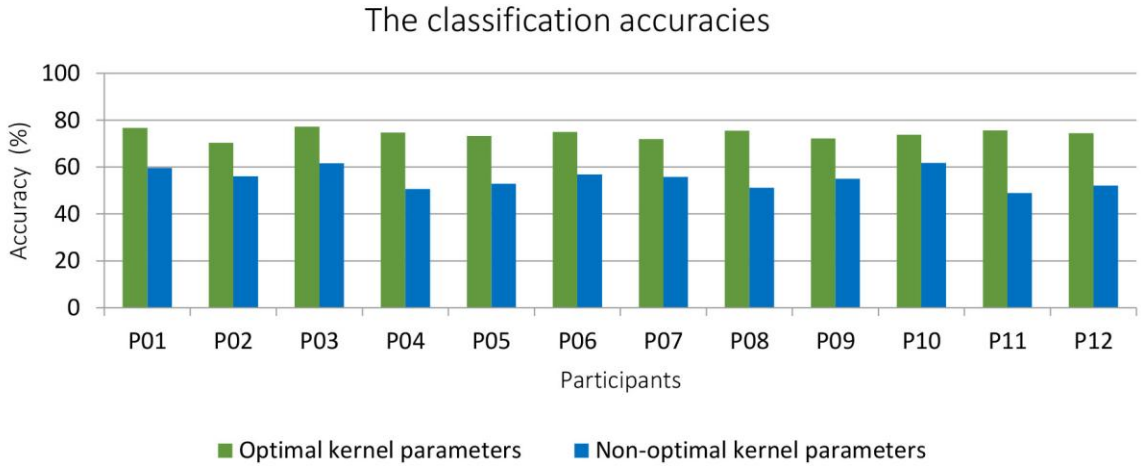

Figure 8.2: (A) The average classification accuracies of REST versus MI-GRASP versus MI-ELBOW by applying the proposed method using RBF kernel for optimal and non-optimal parameters. (B) The classification accuracies of REST versus MI-GRASP versus MI-ELBOW by applying the proposed method using optimal and non-optimal parameters for each participant.

Table 8.2: The average cross-validation accuracy of the proposed method, the optimal *c* and γ values for each participant are presented.

Participant	Selected *c*	Selected γ	Proposed Method Accuracy (%)
Participant P01	10	2.5	73.7 ± 3.1
Participant P02	10	2.5	68.3 ± 2.6
Participant P03	10	2.4	74.8 ± 3.0
Participant P04	25	2.3	70.9 ± 4.7
Participant P05	40	2.5	66.5 ± 5.4
Participant P06	15	2.5	71.9 ± 3.5
Participant P07	25	2.1	70.0 ± 2.3
Participant P08	10	2.5	71.0 ± 4.1
Participant P09	15	2.3	70.1 ± 3.0
Participant P10	45	1.4	71.8 ± 2.4
Participant P11	25	2.4	69.6 ± 6.1
Participant P12	10	2.4	71.1 ± 4.2

8.4. Conclusion

The overall results of the multi-class classifications were discussed in this chapter. The investigations and the research were discussed in terms of the importance and sensitivity of selecting the parameters. The average accuracy achieved for each participant using the parameters in the selected interval were presented and discussed. The improving EEG interpretation to differentiate between imagery of different types of hand movements, using proposed technique, is clearly defined in the next chapter.

Chapter 9. Proposed Classification Scheme and CSP, FBCSP and Band Power Methods for Upper Extremity Imagery Motor Movement Recognition

9.1. Introduction

This chapter compares the results obtained from addressing objectives 1 and 2 with the results obtained using well-known methods that are widely used in BCI literature. The results obtained using the proposed method, are compared with CSP, FBCSP and band power methods. The content of this chapter was slightly modified from what first appeared in print in:

Tavakolan, M, Frehlick, Z, Yong X-Y, Menon, C (2017) Classifying three imaginary states of the same upper extremity using time-domain feature, PLoS ONE, Vol.12, No3, 18pp.

Tavakolan M, Yong X-Y, Zhang, X, and Menon C (2016) Classification Scheme for Arm Motor Imagery, Journal of Medical and Biological Engineering. Vol 36, No.1, pp 12-21.

9.2. Performance Comparison

Figure 9.1 presents in detail comparison between the proposed method and CSP, FBCSP and band power methods. As it is presented, the pattern recognition accuracy of the proposed method was higher compared with the accuracy of CSP, FBCSP and band power methods for binary classification of REST versus MI-GRASP and REST versus MI-ELBOW.

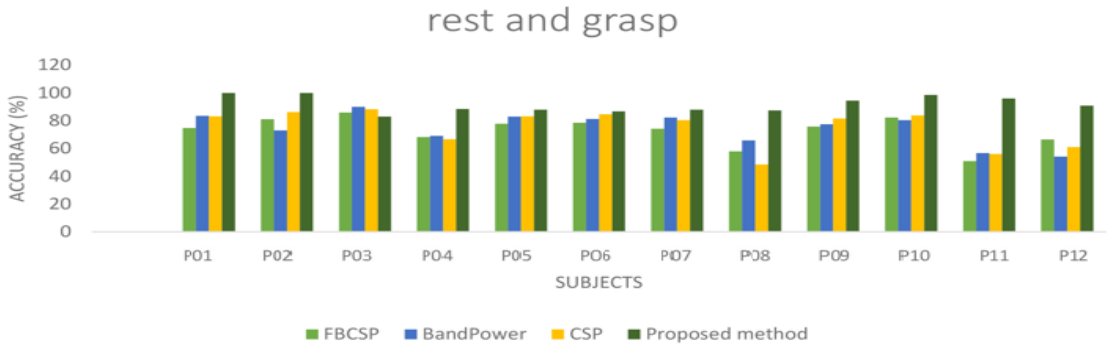

A

B

Figure 9.1: The classification accuracies of the proposed, CSP, FBCSP and band power methods for each individual. (A) REST versus MI-GRASP. (B) REST versus MI-ELBOW.

The average classification accuracies of REST versus MI-GEASP and REST versus MI-ELBOW for each method is presented in Figure 9.2. The average classification accuracy for the proposed method is higher compared to those of the CSP, FBCSP and band power methods. The analysis of variance results show that there were statistically significant differences ($p < 0.01$) between the results obtained using the proposed method and those obtained using the other methods. The average classification accuracy results indicate that the CSP, FBCSP, and band power methods are all powerful and that there is a small difference in their pattern recognition performances.

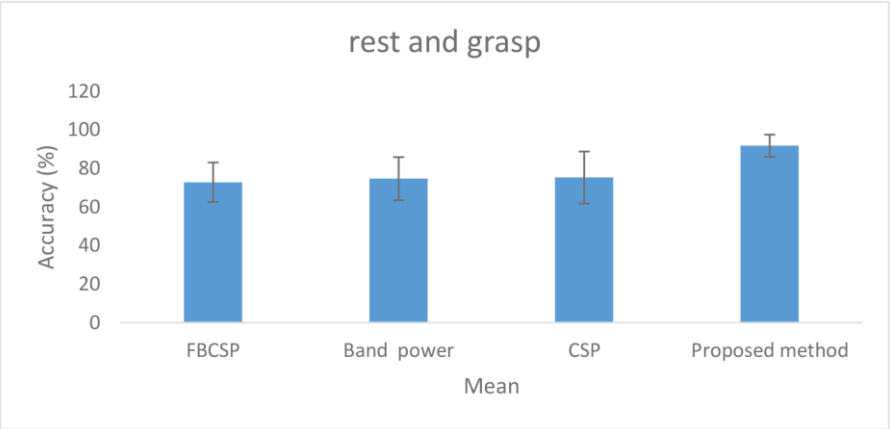

A

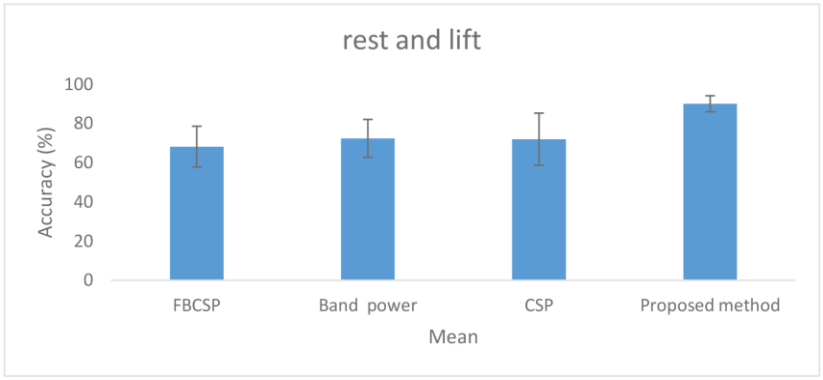

B

Figure 9.2: Average classification accuracies of proposed, CSP, FBCSP, and band power methods. (A) REST versus MI-GRASP. (B) REST versus MI-ELBOW.

The obtained cumulative error rates using the optimal model of the proposed method, CSP, FBCSP and band power methods are presented in Figure 9.3. As it is presented in Figure 9.3, there was relatively low classification error rate for participants P01 and P02 using the CSP, FBCSP and band power pattern recognition models for MI-GRASP and REST classification. The error rate was zero for these participants using the proposed optimal model. The higher cumulative error rates for participants P08, P11 and P12 show that, there was a high classification error rate using the CSP, FBCSP and band power pattern recognition models. The overall error rates was however small and acceptable for these participants using the proposed optimal model, which shows that for BCI applications, these features – classifier can be considered as a potential option for classification.

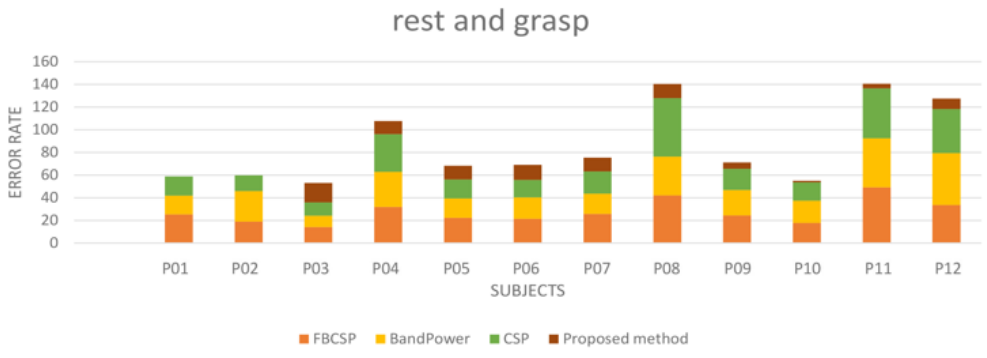

A

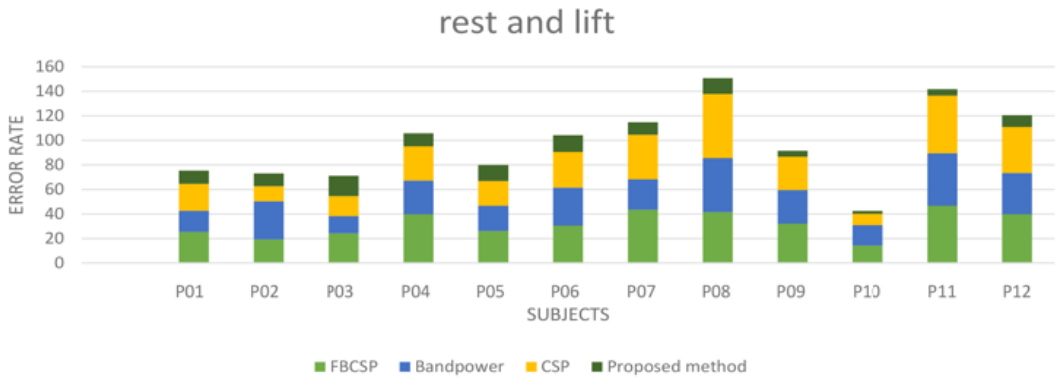

B

Figure 9.3: The cumulative error rates of the proposed, CSP, FBCSP and band power methods for each individual. (A) REST versus MI-GRASP. (B) REST versus MI-ELBOW.

The performance of the proposed method was also compared with those obtained when CSP, FBCSP and band power methods were used for classification of REST versus MI-GRASP versus MI-ELBOW. The results show that the proposed scheme outperformed the other methods for each individual. Figure 9.4 illustrates the comparison of the performance of the proposed method with that obtained when CSP, FBCSP and band power methods were used for each individual.

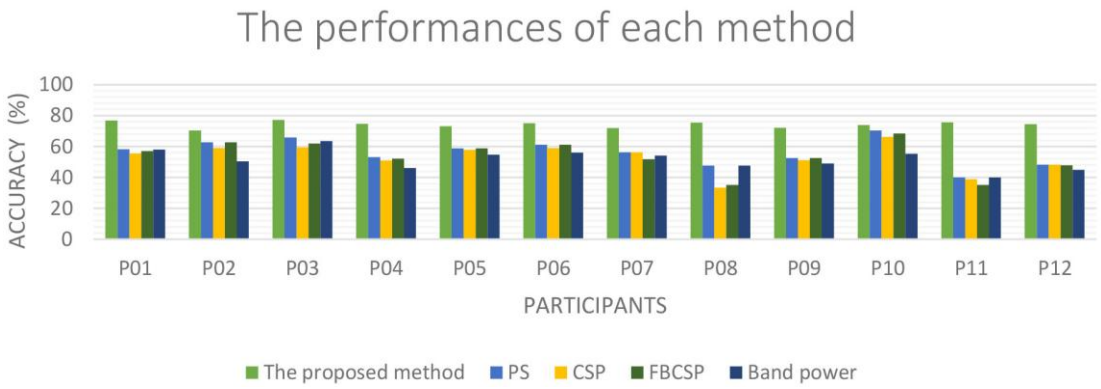

Figure 9.4: The classification accuracies of REST versus MI-GRASP versus MI-ELBOW by applying the proposed method, CSP, FBCSP, PS and band power methods.

The average classification accuracies in addition to the maximum and minimum accuracies are presented in Figure 9.5 A and B for each method. Figure 9.5A shows that the accuracy obtained from the proposed method was on average higher compared to those obtained from other methods. CSP, FBCSP and band power methods achieved an

average classification accuracy of 53 ± 9.3%, 53.7 ± 10.4% and 51.7 ± 6.5% respectively for the classification of REST versus MI-GRASP versus MI-ELBOW. To compare the results of the different methods, a pairwise statistical analysis between the proposed method and each of the well-known methods based on CSP, FBCSP, band power, and PS was performed. ANOVA was used since the data were normally distributed as assessed by Shapiro-Wilk Test ($p > 0.05$) [99]. The analysis showed that the means of the performance of the BCI for the proposed method and the previously mentioned methods were statistically significant ($p < 0.01$).

For the 3-class problem investigated in this study the best classification accuracy (i.e., an average of 74.2% ± 2.1%) was achieved by the proposed scheme (see Figure 9.5 B). The maximum accuracy achieved was 77.2% (participant P03) using the proposed method whereas the lowest accuracy was 33.4% (participant P08) using the CSP method. The performance of the FBCSP method was very close to that of the CSP method (i.e., 35.2% for participant P08).

Figure 9.6 presents the cumulative error rates for each participant. Small cumulative error rate is presented for participant P10 for REST, MI-GRASP, and MI-ELBOW classification using different methods. For this participant, a relatively low classification error rate was achieved in the CSP, FBCSP and band power. However, the error rate was the lowest for this participant when the proposed optimal model was used. Higher cumulative error rates were observed in participants P08, P11 and P12 (see Figure 9.6). The overall error rate was lower for these participants when the proposed optimal model was used. However, high classification error rates were obtained when using other methods. These results show that for BCI applications, the proposed method can be considered as a potential option.

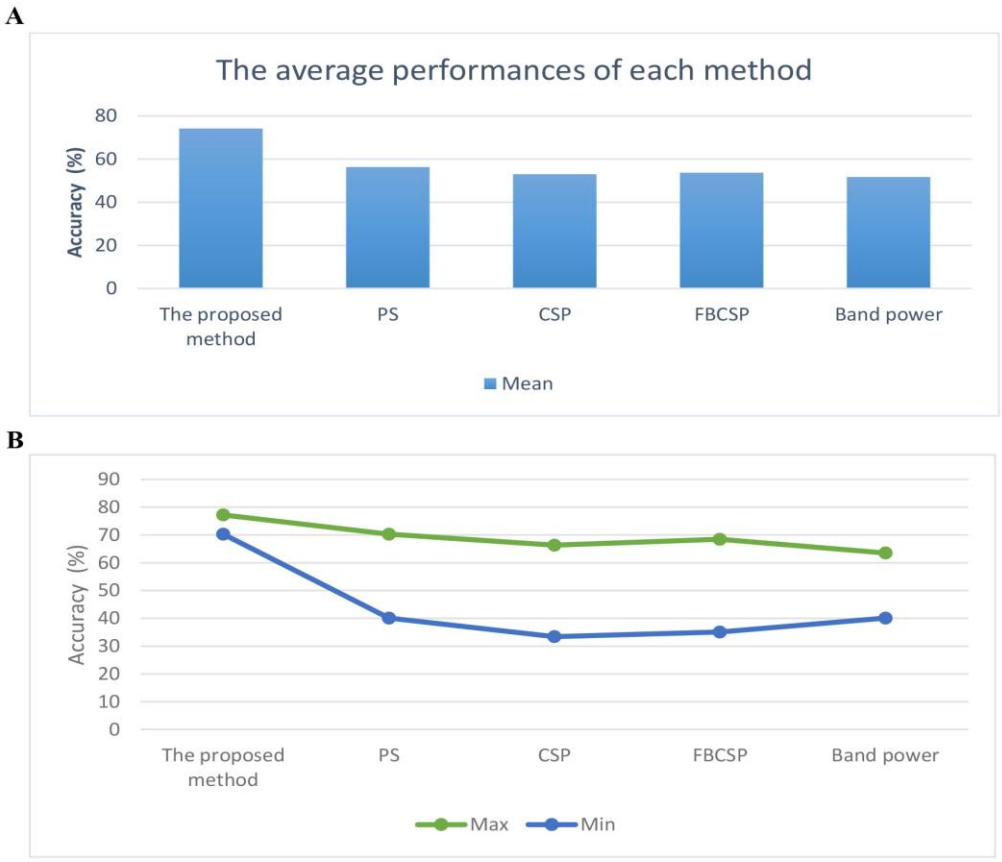

Figure 9.5: (A) The average classification accuracies of REST versus MI-GRASP versus MI-ELBOW by applying the proposed method, CSP, FBCSP, PS and band power methods. (B) The minimum and maximum performance obtained by applying the proposed method, CSP, FBCSP, PS and band power methods.

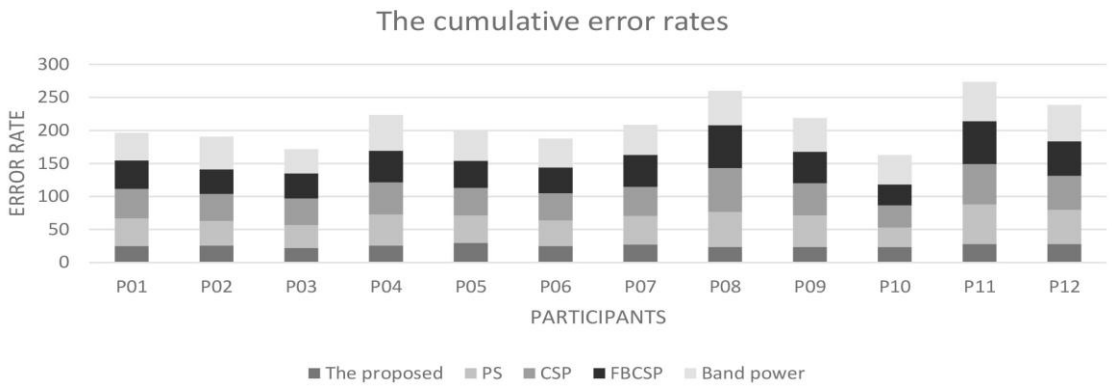

Figure 9.6: The cumulative error rates of the proposed method, CSP, FBCSP, PS and band power methods for each individual.

The ability of predicting different postures of the upper extremity using EEG was investigated. The obtained results confirmed that the EEG data captured from the EGI's Geodesic sensor net produced distinct patterns for the selected upper-extremities postures of the imagined motor movement tasks. The data were reasonably separable and well modelled by the extracted features and optimal SVM model. Binary-class BCI system was proposed that discriminates EEG signals corresponding to REST versus MI-GRASP and REST versus MI-ELBOW movements within the same limb. Multi-class classification study was also designed to assess the performance of the proposed classification scheme. The patterns of MI-GRASP, MI-ELBOW and REST were successfully recognized. An acceptable classification performance was obtained for the classification of arm motor imagery using the proposed method.

The results obtained from the proposed BCI are promising. The obtained results therefore point out that the proposed scheme has potential for providing intention of the participant during imaginary functional movements. The proposed method could potentially be used in BCI-driven assistive devices, such as portable exoskeletons for assisting with arm movements. The proposed three-class BCI could for instance increase the controlled number of degrees of freedom of the robotic device paired with functional electrical stimulation (FES) designed in MENRVA laboratory for assistive purposes or for stroke rehabilitation [24]. In case of assistance, for example, the participant could imagine "to move her/his elbow" to control the robotic device, which can assist with extending the arm when reaching out for an object, and imagine instead "grasping with her/his hand" to activate FES, which can assist with grasping the targeted object. For rehabilitation purposes, a similar strategy could be implemented to assist with repetitions of task-specific exercises (e.g. picking up a bean bag and place it on a different location). Task-specific training after stroke has been shown to produce long-lasting cortical reorganization compared to traditional stroke rehabilitation and potential for better functional outcomes [100-102].

9.3. Conclusion

The differences in the results for imagined movements were discussed in this chapter. The investigations and the research were discussed in terms of the features

used and the accuracies of the results. This chapter compared the results obtained from addressing objectives 1 and 2 with the results obtained using well-known methods that are widely used in BCI literature. The next chapter concludes the research and future works are suggested.

Chapter 10. Conclusion

The overall goal of this thesis, improving EEG classification accuracy of single limb imaginary movements was met by addressing the following objectives:

Objective 1: Binary classification

1.1: Rest versus motor imagery of grasp

1.2: Rest versus motor imagery of elbow flexion and extension

Objective 2: Multi-class classification - Rest versus motor imagery of grasp versus motor imagery of elbow flexion and extension

Objective 1 was met by optimizing two different binary classification models for identifying rest state versus motor imagery of grasp (objective 1.1) and identifying rest state versus motor imagery of elbow flexion and extension (objective 1.2). The AR model coefficients, RMS amplitude, and WL were extracted from the acquired EEG signals. The SVM classifier was used for discriminating the REST and imagined arm movements of participants. Selecting optimized kernel function parameters and appropriate features were addressed as the key factors to obtaining satisfactory recognition results in chapter 7 and chapter 8.

Objective 2 was addressed in chapter 8 which the optimal multi-class classification models were built for each participant. The possibility of associating EEG patterns with the imagining of arm movements was investigated. The identified classes were rest versus motor imagery of grasp versus motor imagery of elbow flexion and extension. The obtained results support the hypothesis that successful pattern recognition can be achieved when discriminating imagined arm movements of users in vital activities of daily living.

Chapter 9 compares the obtained binary-classification results of the Objective 1.1 and objective 1.2 with the well-known methods, which are widely used in the literature. Average accuracies of 91.8 ± 5.8 % and 90 ± 4.1 % were obtained for distinguishing rest versus grasping and rest versus elbow flexion. The results show that the proposed

scheme provides 18.9 %, 17.1 %, and 16.5 % higher classification accuracies for distinguishing rest versus grasping and 21.9 %, 17.6 %, and 18.1 % higher classification accuracies for distinguishing rest versus elbow flexion compared with those obtained using filter bank common spatial pattern, band power, and common spatial pattern methods.

Objective 2 was also addressed in chapter 9. For the case of multi-class classification, it was shown that the investigated method achieved an average accuracy of 74.2%, which is at least 20.0% higher compared to other methods. The implemented pattern recognition strategy identified various imagined arm movements within the same limb. The pattern recognition strategy outperformed methods that are widely used in the literature such as CSP, FBCSP, and band power methods.

In future work, The feasibility of classifying the EEG signals related to rest and the imaginary grasp and elbow movements within the same limb will be investigated among individuals with neurological disorders, including individuals with stroke with different levels of impairments. A higher density EEG system would be used in order to obtain higher resolution maps especially close to the motor cortex. In fact, the investigated motor imagery tasks activate regions that have very close representations on the motor cortex area of the brain [13, 14]. Real-time classification will be conducted to validate that acceptable performance can be obtained.

Future research will focus on developing a hybrid human machine interface system that combines the proposed EEG-based BCI with EMG placed on the arm to further engage individuals with a hemiparetic arm resulting from a stroke for facilitating motor recover of their arm.

References

[1] E. Buch, C. Weber, L. G. Cohen, C. Braun, M. A. Dimyan, T. Ard, J. Mellinger, A. Caria, S. Soekadar, A. Fourkas and N. Birbaumer, “Think to move: a neuromagnetic brain-computer interface (BCI) system for chronic stroke,” *Stroke*, 39: 910-917, 2008.

[2] F. Lotte, M. Congedo, A. Lécuyer, F. Lamarche and B. Arnaldi, “A review of classification algorithms for EEG-based brain-computer interfaces,” *J. Neural Eng.*, 4: R1-R13, 2007.

[3] S. Marcel and J. D. R. Millán, “Person authentication using brainwaves (EEG) and maximum a posteriori model adaptation,” *IEEE Trans. Pattern Anal. Mach. Intell.*, 29: 743-752, 2007.

[4] K. Brigham and B. V. Kumar, “Subject identification from electroencephalogram (EEG) signals during imagined speech,” *Proc. IEEE 4th Int. Conf. Biometrics: Theory Applications and Systems*, 1-8, 2010.

[5] R. Palaniappan, “Two-stage biometric authentication method using thought activity brain waves,” *Int. J. Neural Syst.*, 18: 59-66, 2008.

[6] McFarland D J, Anderson C W, Muller K R, Schl¨ogl A and Krusienski D J 2006 BCI meeting 2005—workshop on BCI signal processing: feature extraction and translation *IEEE Trans. Neural Syst. Rehabil. Eng.* 14 135–8

[7] Dornhege G, Blankertz B, Curio G andM¨uller K R 2002 Combining features for BCI *Advances in Neural Information Processing Systems (NIPS 02)* vol 15 ed S Becker, S Thrun and K Obermayer (Cambridge, MA: MIT Press) pp 1115–2

[8] R. Palaniappan, “Utilizing gamma band to improve mental task based brain-computer interface design,” *IEEE Trans. Neural Syst. Rehabil. Eng.*, 14: 299-303, 2006.

[9] C. R. Hema, M. P. Paulraj, R. Nagarajan, S. Yaacob and A. H. Adom, “Fuzzy Based Classification of EEG Mental Tasks for a Brain Machine Interface,” *Proc. IEEE 3rd Int. Conf. Intelligent Information Hiding and Multimedia Signal Processing*, 1: 53-56, 2007.

[10] P. F. Diez, V. Mut, E. Laciar, A. Torres and E. Avila, “Application of the empirical mode decomposition to the extraction of features from EEG signals for mental task classification,” *Proc*. *IEEE 31st Int*. *Conf*. *Engineering in Medicine and Biology Society*, 2579-2582, 2009.

[11] N. J. Huan and R. Palaniappan, “Classification of mental tasks using fixed and adaptive autoregressive models of EEG signals,” *Proc*. *IEEE 26th Int*. *Conf*. *Engineering in Medicine and Biology Society*, 1: 507-510, 2004.

[12] Pfurtscheller G, Neuper C (2001) Motor imagery and direct brain-computer communication. In: Proceedings of the IEEE. 7, pp. 1123–1134.

[13] Sanes JN, Donoghue JP, Thangaraj V, Edelman RR, Warach S. Shared neural substrates controlling hand movements in human motor cortex. Science. 1995; 268 (5218):1775–1777.

[14] Plow EB, Arora P, Pline MA, Binenstock MT, Carey JR. Within-limb somatotopy in primary motor cortex– revealed using fMRI. Cortex. 2010; 46(3):310–321.

[15] Vuckovic A, Sepulveda F (2008) Delta band contribution in cue based single trial classification of real and imaginary wrist movements. Medical Biological Engineering Computing 46: 529–539.

[16] Ghani F, Sultan H, Anwar D, Farooq O, Khan YU (2013) Classification of wrist movements using EEG signals. Journal of Next Generation Information Technology (JNIT) 4: 29–39.

[17] Navarro I, Sepulveda F, Hubais B (2005) A comparison of time, frequency and ICA based features and five classifiers for wrist movement classification in EEG signals. In: IEEE EMBS. Shanghai, China, pp. 2118–2115.

[18] Prasad G, Herman P, Coyle D,McDonough S, Crosbie J (2010) Applying a brain-computer interface to support motor imagery practice in people with stroke for upper limb recovery: a feasibility study. Journal of Neuroengineering and Rehabilitation 7: 1–17.

[19] Ortner R, Irimia DC, Scharinger J, Guger C (2012) A motor-imagery based brain-computer interface for stroke rehabilitation. Annual Review of Cybertherapy and Telemedicine 181: 319–323.

[20] Ang KK, Guan C, Chua KSG, Ang BT, Kuah C, et al. (2009) A clinical study of motor imagerybased brain-computer interface for upper limb robotic rehabilitation. In: EMBS 2009. Minnesota, USA, pp. 5981–5984.

[21] Ang KK, Guan C, Chua KSG, Ang BT, Kuah C, et al. (2010) Clinical study of neurorehabilitation in stroke using EEG-based motor imagery brain-computer interface with robotic feedback. In: EMBS 2010. Buenos Aires, Argentina, pp. 5549–5552.

[22] Ang KK, Guan C, Chua KSG, Ang BT, Kuah C, et al. (2011) A large clinical study on the ability of stroke patients to use an EEG-based motor imagery brain-computer interface. Clinical EEG and Neuroscience 42: 253–258.

[23] Yong, X., Menon, C. (2015). EEG Classification of Different Imaginary Movements within the Same Limb. *PloS one*, *10*(4).

[24] Looned R, Webb J, Xiao ZG, Menon C (2014) Assisting drinking with an affordable BCI-controlled wearable robot and electrical stimulation: a preliminary investigation. Journal of NeuroEngineering and Rehabilitation 11: 1–13.

[25] Wolpaw J R, Birbaumer N, McFarland D J, Pfurtscheller G, Vaughan T M. *Brain-computer interfaces for communication and control*. Clinical Neurophysiology, Vol 113, 2002, pp 767 – 791.

[26] Mason S G, Birch G E. *A general Framework for Brain Computer Interface Design*. IEEE Transactions on Neural Systems and Rehabilitation Engineering, Vol 11, March 2003, pp 70 – 85.

[27] Gray, F. J. (2002) *Anatomy for the medical clinician*, first edition, Shannon Books Pty Ltd, Victoria, Australia.

[28] G. D. Schott, “Penfield’s homunculus: a note on cerebral cartography,” Journal of Neurology, Neurosurgery and Psychiatry, vol. 56, no. 4, pp. 329–333, 1993.

[29] Carlson, N. R. (2002b) ‘Structure and Functions of the Nervous System’, *Foundations of physiological psychology*, Vol. 5th ed. Issue 3. Boston, Mass. London: Allyn and Bacon.

[30] Sanei, S. and Chambers, J. A. (2007) *EEG Signal Processing*, John Wiley & Sons, Ltd., 2007.

[31] Purves, D., Augustine, G.J., Fitzpatrick, D., Katz, L.C. Lamantia, A.S. and McNamara, J.O. (2004) *Neuroscience*, Sinauer associates, third edition, Inc. Publishers, Sunderland, Massachusetts, USA.

[32] Khokhar, Z.O., Xiao Z.G., and Menon, C (2010), Surface EMG pattern recognition for real-time control of a wrist exoskeleton, BioMedical Engineering OnLine 2010, Vol. 9, No. 41.

[33] Yuan H, Liu T, Szarkowski R, Rios C, Ashe J, He B. Negative covariation between task-related responses in alpha/beta-band activity and BOLD in human sensorimotor cortex: an EEG and fMRI study of motor imagery and movements. Neuroimage. 2010; 49(3):1–21. doi: 10.1016/j.neuroimage.2009.10. 028

[34] Wolpaw JR, Birbaumer N, McFarland DJ, Pfurtscheller G, Vaughan TM. Brain-computer interface for communication and control. Clin Neurophysiol. 2002; 113:767–791. doi: 10.1016/S1388-2457(02) 00057-3 PMID: 12048038.

[35] Bashashati A, Fatourechi M, Ward R K, Birch G E. *A survey of signal processing algorithms in brain-computer interfaces based on electrical brain signals*. Journal of Neural Engineering, Vol 4, 2007, pp R32 – R57.

[36] Vuckovic, A. *Non-invasive BCI: How far can we get with motor imagination?*. Clinical Neurophysiology, Vol 120, 2009, pp 1422-1423.

[37] Hashimoto, Y., Ushiba, J., Kimura, A., Liu, M., & Tomita, Y. (2010). Correlation between EEG-EMG coherence during isometric contraction and its imaginary execution. *Acta Neurobiol Exp (Wars)*, *70*(1), 76-85.

[38] Khokhar, Z.O., Xiao Z.G., and Menon, C (2010), Surface EMG pattern recognition for real-time control of a wrist exoskeleton, BioMedical Engineering OnLine 2010, Vol. 9, No. 41.

[39] Tavakolan M, Xiao ZG and MenonC (2011) A preliminary investigation assessing the viability of classifying hand postures in seniors, BioMedical Engineering Online, Vol. 10, No.79 (16pp)

[40] Tavakolan, M, Khokhar, Z.O., Menon, C (2010) Classification of surface electromyography signals in seniors: a case study, IEEE/RA/EMB/IFMBE International Conference on Applied Bionics and Biomechanics, Venice, Italy

[41] Tavakolan, M, Khokhar, Z.O., Menon, C (2010) Pattern Recognition for Estimation of Wrist Torque Based on Forearm Surface Electromyography Signals, IEEE/RA/EMB/IFMBE International Conference on Applied Bionics and Biomechanics, Venice, Italy

[42] Khezri M, Jahed M: Real-time intelligent pattern recognition algorithm for surface EMG signals. Biomed Eng Online 2007, 6:45.

[43] Castellini C, Smagt PVD: Surface EMG in advanced hand prosthetics. Biological cybernetics Springer-Verlag 2008.

[44] Oskoei MA, Hu H: Support vector machine-based classification scheme for myoelectric control applied to upper limb. IEEE Trans Biomed Eng 2008, 55:1956-1965.

[45] A. Khorshidtalab, M. J. E. Salami and M. Hamedi. “Robust classification of motor imagery EEG signals using statistical time–domain features,” *Physiol. Meas.,* 34: 1563,2013.

[46] A. Khorshidtalab, M.J.E. Salami and M. Hamedi, “Evaluation of timedomain features for motor imagery movements using FCM and SVM,” In Computer Science and Software Engineering, International Joint Conference on IEEE. pp. 17-22, 2012.

[47] V. Vapnik, “The support vector method of function estimation,” 55-85, 1998.

[48] Hsu CW, Chang CC, Lin CJ: A practical guide to support vector classification. Technical report. Department of Computer Science and Information Engineering, National Taiwan University, Taipei, Taiwan 2003

[49] C. M. Bishop, *Pattern Recognition and Machine Learning.* Springer, 2006.

[50] Morley JE: The top ten hot topics in aging. Journal of Gerontology Medical Sciences 2004, 59:24-33.

[51] Khokhar ZO, Xiao ZG, Sheridan C, Menon C: A Novel wrist/rehabilitation device. Proceedings of the 13th IEEE International Multitopic Conference, 14-15 Dec., Islamabad 2009 80-85.

[52] Reaz MBI, Hussain MS, Yasin FM: Techniques of EMG signal analysis: detection, processing, classification and applications. Biological Proceedings Online 2006, 8:11-35.

[53] The SmartHand project. 2007 [http://www.elmat.lth.se/~smarthand].

[54] The CyberHand project. 2007 [http://www.cyberhand.org].

[55] Otto Bock SensorHand hand prothesis. 2010 [http://www.ottobock.com/cps/rde/xchg/ob_com_en/hs.xsl/3652.html].

[56] The iLimb prosthetic hand. 2007 [http://www.touchbionics.com].

[57] Henry M, Sheridan C, Khokhar ZO, Menon C: Towards the development of a wearable rehabilitation device for stroke survivors. Proceedings of IEEE Toronto International Conference 26-27 Sep., Toronto 2009.

[58] Maier MA, Raymond MCH: EMG activation patterns during force production in precision grip. 1. Contribution of 15 finger muscles to isometric force. Exp Brain Res 1995, 103:108-122.

[59] Cuevas FJV, Zajac FE, Burgar CG: Large index-fingertip forces are produced by subject independent patterns of muscle excitation. J Biomechanics 1998, 31:693-703.

[60] Cuevas FJV: Predictive modulation of muscle coordination pattern magnitude scales fingertip force magnitude over the voluntary range. J Neurophysiology 2000, 83:1469-1479.

[61] Parker P, Englehart K, Hudgins B: Myoelectric Signal Processing for Control of Powered Limb Prostheses. Journal of Electromyography and Kinesiology 2006, 16:541-548.

[62] Clancy EA, Hogan N: Theoretic and Experimental Comparison of Root-Mean-Square and Mean-Absolute-Value Electromyogram Amplitude Detectors. Proc. nineteenth Annu. Int. Conf. IEEE Engineering in Medicine and Biology Society (EMBS '97) 1997, 3:1267-1270.

[63] Chu JU, Moon I, Lee YJ, Kim SK, Mun MS: A supervised feature-projection-based real-time EMG pattern recognition for multifunction myoelectric hand control. IEEE/ASME Transactions on Mechatronics 2007, 12:282-290.

[64] Englehart K, Hudgins B, Parker PA, Stevenson M: Classification of the myoelectric signal using time-frequency based representations. Medical Eng & Physics 1999, 21:431-438.

[65] Yoshikawa M, Mikawa M, Tanaka K: A Myoelectric interface for robotic hand control using support vector machine. Proceedings of the IEEE/RSJ International Conference on Intelligent Robots and Systems: 29 October - 2 November 2007; San Diego 2007, 2723-2728.

[66] Saunders C, Stitson MO, Weston J, Bottou L, Sch¨olkopf B, Smola A: Support vector machine reference manual. Technical Report CSD-TR-98-03, Royal Holloway, University of London, London 1998.

[67] Liu YH, Huang HP, Weng CH: Recognition of electromyographic signals using cascaded kernel learning machine. IEEE/ASME Trans Mechatronics 2007, 12:253-264.

[68] Bitzer S, Smagt PVD: Learning EMG control of a robotic hand: towards active prosthesis. Proceedings of the IEEE International Conference on Robotics and Automation: 15-19 May 2006; Orlando 2006, 2819-2823.

[69] Chan ADC, Englehart KB: Continuous myoelectric control for powered prosthesis using hidden markov models. IEEE Trans Biomed Eng 2005, 52:121-124.

[70] Soares A, Andrade A, Lamounier E, Carrijo R: The development of a virtual myoelectric prosthesis controlled by an EMG pattern recognition system based on neural networks. Journal of Intelligent Information Systems 2003, 21:127-141.

[71] Englehart K, Hudgins B, Parker P: A wavelet-based continuous classification scheme for multifunction myoelectric control. IEEE Trans Biomed Eng 2001, 48:302-311.

[72] Karlik B, Tokhi MO, Alci M: A fuzzy clustering neural network architecture for multifunction upper-limb prosthesis. IEEE Transactions on Biomedical Engineering 2003, 50:1255-1261.

[73] Inoue T, Abe S: Fuzzy support vector machines for pattern classification. Proceedings of International Joint Conference on Neural Networks(IJCNN '01) 2001, 2:1449-1454.

[74] Park SH, Lee SP: EMG pattern recognition based on artificial intelligence techniques. IEEE Trans on Rehab Eng 1998, 6:400-405.

[75] Khezri M, Jahed M: Real-time intelligent pattern recognition algorithm for surface EMG signals. Biomedical Engineering Online 2007, 6:45.

[76] Chan FHY, Yang YS, Lam FK, Zhang YT, Parker PA: Fuzzy EMG classification for prosthesis control. IEEE Trans on Rehab Eng 2000, 8:305-311.

[77] Chu JU, Lee YJ: Conjugate-prior-penalized learning of Gaussian mixture models for multifunction myoelectric hand control. IEEE Trans Neural Sys and Rehab Eng 2009, 17:287-297.

[78] Englehart K, Hudgins B: A robust, real-time control scheme for multifunction myoelectric control. IEEE Trans Biomed Eng 2003, 50:848-854.

[79] Chu JU, Moon I, Mun MS: A real-time EMG pattern recognition system based on linear-nonlinear feature projection for a multifunction myoelectric hand. IEEE Trans Biomed Eng 2006, 53:2232-2239.

[80] Carmeli E, Patish H, Coleman R: The Aging Hand, Journal of Gerontology. Medical Sciences 2003, 58A:146-152.

[81] SENIAM Project. [http://www.seniam.org].

[82] Lew HL, TSAI SJ: Pictorial guide to muscles and surface anatomy. In Johnson's practical electromyography.. 4 edition. Edited by: Pease WS, Lew HL, Johnson EW. Lippincott Williams 2007:145-212.

[83] Luca CJD: Surface electromyography: detection and recording. 2002 by DelSys Incorporated.

[84] Mital A, Pennathur A: Musculoskeletal overexertion injuries in the United States: mitigating the problem through ergonomics and engineering interventions. Journal of Occupational Rehabilitation 1999, 9:115-149.

[85] Santello M, Soechting JF: Force synergies for multifingered grasping. Exp Brain Res 2000, 133:457-467.

[86] Electrical Geodesics I (2007) Geodesic sensor net technical manual. Technical report, Electrical Geodesics, Inc.

[87] Mulert C, Seifert C, Leicht G, Kirsch V, Ertl M, Karch S, Moosmann M, Lutz J, Möller HJ, Hegerl U, Pogarell O. Single-trial coupling of EEG and fMRI reveals the involvement of early anterior cingulate cortex activation in effortful decision making. Neuroimage. 2008 Aug 1;42(1):158-68.

[88] Tucker DM. Spatial sampling of head electrical fields: the geodesic sensor net. Electroencephalography and clinical neurophysiology. 1993 Sep 30;87(3):154-63.

[89] Liu Q, Balsters JH, Baechinger M, van der Groen O, Wenderoth N, Mantini D. Estimating a neutral reference for electroencephalographic recordings: the importance of using a high-density montage and a realistic head model. Journal of neural engineering. 2015 Aug 26;12(5):056012.

[90] Electrical Geodesics I. Net Amps 400 Series Amplifiers. http://www.egi.com.

[91] Pfurtscheller G, da Silva FHL (1999) Event-related EEG/MEG synchronization and desynchronization: basic principles. Clin Neurophysiol 110: 1842–1857.

[92] Dornhege G, Blankertz B, Krauledat M, Losch F, Curio G, et al. (2005) Optimizing spatio-temporal filters for improving Brain-Computer Interfacing. In: Platt J, editor, Advances in Neural Inf. Proc. Systems (NIPS05). Vancouver, Canada, volume 18, pp. 315–322.

[93] Ramoser H, M¨uller-Gerking J, Pfurtscheller G (2000) Optimal spatial filtering of single trial EEG during imagined hand movement. IEEE Trans Rehabil Eng 8: 441–447.

[94] Wang Y, Gao S, Gao X (2005) Common spatial pattern method for channel selection in motor imagery based Brain-computer Interface. In: Engineering in Medicine and Biology Society, 2005. IEEE-EMBS 2005. 27th Annual International Conference of the IEEE. pp. 5392–5395.

[95] Ang KK, Chin CY, Zhang H, Guan C. Filter bank common spatial pattern (FBCSP) in brain-computer interface. In: IEEE International Joint Conference on Neural Networks. Hong Kong; 2008. p. 2390–2397.

[96] B. Blankertz, T. Ryota, L. Steven, K. Motoaki and K. R. Muller, “Optimizing spatial filters for robust EEG single-trial analysis, ”*Signal Process. Mag., IEEE,* 25: 41-56, 2008.

[97] K. K. Ang, Z. Y. Chin, C. Wang, C. Guan and H. Zhang, “Filter bank common spatial pattern algorithm on BCI competition IV datasets 2a and 2b,” *Front. Neurosci*. 6: 39. 2012.

[98] Delorme A, Mullen T, Kothe C, Acar ZA, Bigdely-Shamlo N, Vankov A, et al. EEGLAB, SIFT, NFT, BCILAB, and ERICA: new tools for advanced EEG processing. Computational Intelligence and Neuroscience. 2011; 1-12.

[99] Hollander M, Wolfe DA, Chicken E. Nonparametric Statistical Methods. 3rd ed. Wiley; 2013.

[100] Hubbard IJ, Parsons MW, Neilson C, Carey LM. Task-specific training: evidence for and translation to clinical practice. Occupational Therapy International. 2009; 16(3–4):175–189.

[101] Rensink M, Schuurmans M, Linderman E, Hafsteinsdottir T. Task-oriented training in rehabilitation after stroke: systematic review. Journal of Advanced Nursing. 2008; 65(4):737–754.

[102] Classen J, Liepert J, Wise SP, Hallet M, Cohen LG. Rapid plasticity of human cortical movement representation induced by practice. Journal of Neurophysiology. 1998; 79(2): 1117-1123.